The Astrophysical Journal, 670:173–189, 2007 November 20

MULTIWAVELENGTH STUDY OF MASSIVE GALAXIES AT $z \sim 2$. II. WIDESPREAD COMPTON-THICK ACTIVE GALACTIC NUCLEI AND THE CONCURRENT GROWTH OF BLACK HOLES AND BULGES

E. Daddi,[1] D. M. Alexander,[2] M. Dickinson,[3] R. Gilli,[4] A. Renzini,[5] D. Elbaz,[1] A. Cimatti,[6] R. Chary,[7] D. Frayer,[7] F. E. Bauer,[8] W. N. Brandt,[9] M. Giavalisco,[10] N. A. Grogin,[11] M. Huynh,[7] J. Kurk,[12] M. Mignoli,[4] G. Morrison,[13,14] A. Pope,[15] and S. Ravindranath[16]

Received 2007 May 19; accepted 2007 July 22

ABSTRACT

Approximately 20%–30% of $1.4 \lesssim z \lesssim 2.5$ galaxies with $K_{\rm Vega} < 22$ detected with *Spitzer* MIPS at 24 μm show excess mid-IR emission relative to that expected based on the rates of star formation measured from other multiwavelength data. These galaxies also display some near-IR excess in *Spitzer* IRAC data, with an SED peaking longward of 1.6 μm in the rest frame, indicating the presence of warm dust emission usually absent in star-forming galaxies. Stacking *Chandra* data for the mid-IR excess galaxies yields a significant hard X-ray detection at rest-frame energies >6.2 keV. The stacked X-ray spectrum rises steeply at >10 keV, suggesting that these sources host Compton-thick AGNs with column densities $N_{\rm H} \gtrsim 10^{24}$ cm^{-2} and an average, unobscured X-ray luminosity $L_{2-8\,\rm keV} \approx (1-4) \times 10^{43}$ ergs s^{-1}. Their sky density ($\sim$3200 deg^{-2}) and space density ($\sim 2.6 \times 10^{-4}$ Mpc^{-3}) are twice those of X-ray–detected AGNs at $z \approx 2$, and much larger than those of previously known Compton-thick sources at similar redshifts. The mid-IR excess galaxies are part of the long sought after population of distant heavily obscured AGNs predicted by synthesis models of the X-ray background. The fraction of mid-IR excess objects increases with galaxy mass, reaching $\sim$50%–60% for $M \sim 10^{11}\ M_{\odot}$, an effect likely connected with downsizing in galaxy formation. The ratio of the inferred black hole growth rate from these Compton-thick sources to the global star formation rate at $z = 2$ is similar to the mass ratio of black holes to stars in local spheroids, implying concurrent growth of both within the precursors of today's massive galaxies.

Subject headings: galaxies: active — galaxies: evolution — galaxies: formation — X-rays: galaxies

Online material: color figures

1. INTRODUCTION

Active galactic nuclei (AGNs) and galaxies are intimately connected. It is generally thought that virtually all nearby early-type galaxies (and perhaps all relatively massive galaxies) contain a supermassive central black hole (BH), indicating that all massive galaxies may have experienced an AGN phase in their past (Kormendy & Richstone 1995; Magorrian et al. 1998). Moreover, remarkably tight correlations have now been unveiled between central supermassive BHs and the mass or velocity dispersion of the bulge in their host galaxies (Ferrarese & Merritt 2000; Gebhardt et al. 2000), with typical mass ratio $M_{\rm BH}/M_{\rm bulge} \sim (1-2) \times 10^{-3}$ (e.g., McLure & Dunlop 2001; Ferrarese et al. 2006). This suggests but does not establish that AGNs and star formation activity may have been concurrent. The origin of these correlations is in fact not entirely clear and has been the subject of active debate during recent years. It appears to be connected to the positive feedback that the BH can exercise on its host galaxy, becoming effective if the BH exceeds some critical mass limit and thus luminosity (Silk & Rees 1998; Di Matteo et al. 2005; Springel et al. 2005; Schawinski et al. 2006). If the energetic emission from accretion around the BH is large enough, the galaxy can be cleared out of its gas via either heating (e.g., Ciotti & Ostriker 1997, 2007) or accretion-related outflows as in broad absorption line (BAL) quasars (e.g., Chartas et al. 2007), thereby preventing further gas accretion.

In order to probe BH growth in the distant universe, efficient tracers of AGN activity are needed. Obtaining a complete census of active galaxies is complicated due to AGN obscuration by circumnuclear material. During the formation epochs of galaxies, it can be well expected that a greater abundance of gas and its chaotic motions due to merging and interactions cause the typical AGN obscuration to be much larger than locally. In that case, a substantial fraction of the cosmic BH growth history could be hidden from view and not yet taken into account. It is also currently unknown if the "unification paradigm" describing the AGN phenomenon (e.g., Antonucci 1993; Urry & Padovani 1995) holds at high redshift, in particular if the ratio of obscured to unobscured AGNs (or, more accurately, the distribution of obscuring column densities) is the same as observed locally. More generally, the shape of the cosmic X-ray background, with its peak toward 30 keV

[1] Laboratoire AIM, CEA/DSM-CNRS-Universitè Paris Diderot, DAPNIA/SAp, Orme des Merisiers, 91191 Gif-sur-Yvette, France; edaddi@cea.fr.
[2] Department of Physics, Durham University, Durham DH1 3LE, UK.
[3] National Optical Astronomy Observatory, Tucson, AZ 85719.
[4] INAF, Osservatorio Astronomico di Bologna, I-40127 Bologna, Italy.
[5] INAF, Osservatorio Astronomico di Padova, Vicolo Osservatorio 5, I-35122 Padova, Italy.
[6] Dipartimento di Astronomia, Universitá di Bologna, I-40127 Bologna, Italy.
[7] *Spitzer* Science Center, California Institute of Technology, MS 220-6, Pasadena, CA 91125.
[8] Columbia Astrophysics Laboratory, Columbia University, Pupin Laboratories, New York, NY 10027.
[9] Department of Astronomy and Astrophysics, Pennsylvania State University, University Park, PA 16802.
[10] Astronomy Department, University of Massachusetts, Amherst, MA 01003.
[11] School of Earth and Space Exploration, Arizona State University, Tempe, AZ 85287.
[12] Max-Planck-Institut für Astronomie, D-69117 Heidelberg, Germany.
[13] Institute for Astronomy, University of Hawaii, Honolulu, HI 96822.
[14] Canada-France-Hawaii Telescope, Kamuela, HI 96743.
[15] Department of Physics and Astronomy, University of British Columbia, Vancouver, BC V6T 1Z1, Canada.
[16] Inter-University Centre for Astronomy and Astrophysics, Pune University Campus, Pune 411007, Maharashtra, India.

(Marshall et al. 1980), suggests that much of the BH accretion luminosity at substantial redshifts is obscured (e.g., Fabian & Iwasawa 1999).

The deepest X-ray surveys available to date, performed with the *Chandra* satellite in the Chandra Deep Field–South (Giacconi et al. 2002; GOODS-South field, hereafter GOODS-S) and Chandra Deep Field–North (Alexander et al. 2003b; GOODS-North, hereafter GOODS-N) and with *XMM-Newton* (e.g., Hasinger 2004; in the Lockman Hole), resolved most of the X-ray background at energies 0.5–6 keV, but a substantial fraction of the higher energy background remains unresolved (Krivonos et al. 2005; Worsley et al. 2005, 2006; Hickox & Markevitch 2007). Synthesis models have been built (Comastri et al. 1995; Gilli et al. 2001, 2007), showing that in order to account for the high-energy X-ray background, where most of the accretion energy in the universe is being emitted, one has to postulate the existence of substantial populations of high-redshift, heavily obscured, Compton-thick AGNs (with column densities of $N_{\rm H} \gtrsim 10^{24}$ cm^{-2}). Such a population of Compton-thick sources at high redshift still awaits discovery (e.g., Barger et al. 2007). Hard X-ray selection, the best means currently to find such sources at high redshift, is limited by telescope sensitivities and would allow one to find only the brightest sources and with nonextreme column densities (e.g., Brandt & Hasinger 2005). As an example, the archetype Compton-thick AGN NGC 1068, with $L_X > 10^{44}$ ergs s^{-1}, would have a hard X-ray (2–8 keV) flux of only $\sim 7 \times 10^{-18}$ ergs s^{-1} cm^{-2} at $z = 2$, more than an order of magnitude fainter than that of sources detectable in the deepest (2 Ms) *Chandra* survey, in the GOODS-N field.

On the other hand, some of the energy absorbed by the obscuring material is reprocessed and reemitted at longer wavelengths, providing the opportunity to detect these sources via their IR emission. For example, the nucleus of NGC 1068 would have a flux density of 25 μJy at 24 μm if placed at $z = 2$, very faint but still detectable in the ultradeep *Spitzer* MIPS imaging taken as part of GOODS. One of the primary goals of GOODS was indeed the discovery of previously unknown populations of distant AGNs (e.g., Treister et al. 2004) by combining the deepest multiwavelength imaging brought to bear on these fields. Several recent studies have focused on finding distant obscured AGNs by means of mid-IR or far-IR selection, in GOODS and other deep *Spitzer* surveys. For example, selection by means of red IRAC (3.5–8 μm) colors was presented by Lacy et al. (2004) and Stern et al. (2005), and similarly the selection by means of power-law spectral energy distributions (SEDs) over IRAC bands (Alonso-Herrero et al. 2006; Donley et al. 2007) has provided AGN candidate samples with only partial overlap with X-ray–selected sources.

The peak of QSO activity has been established to take place at $z \approx 2$ (e.g., Schmidt 1968; Croom et al. 2004; Hasinger et al. 2005). Therefore, it is quite natural to look for the growth of BHs in massive galaxies at the same epoch. Indeed, the massive $z \sim 2$ galaxies selected at submillimeter wavelengths (SMGs) are undergoing star formation activity and at the same time host luminous AGNs, just the signatures expected for joint stellar BH growth (e.g., Alexander et al. 2005a, 2005b; Borys et al. 2005). However, these sources are relatively rare and appear to represent the most strongly star-forming galaxies at these epochs (e.g., Chapman et al. 2005), and it is important to see if this joint growth is also occurring in more typical massive galaxies at $z \sim 2$.

This paper describes a source population serendipitously discovered while studying the multiwavelength emission properties of distant $1.4 < z < 2.5$ massive star-forming galaxies in the GOODS fields, described in a companion paper (Daddi et al. 2007, hereafter Paper I). As discussed in Paper I, we have built $z \sim 2$ galaxy samples free of detectable AGN activity. A sizable fraction shows distinct mid-IR excess with respect to that expected from star formation activity alone. This property of $z \sim 2$ galaxies implies that the extremely efficient and penetrating 24 μm photometry from *Spitzer* is not always a reliable estimator of the ongoing star formation rates (SFRs) in galaxies, especially in the case of sources with very bright mid-IR luminosities (particularly those encountered at $z \sim 2$ in surveys shallower than GOODS). In this paper we investigate the nature of these mid-IR excess sources in detail. Stacking in the X-ray bands with *Chandra* clearly unveils heavily obscured AGNs, in many cases (or perhaps most cases) with Compton-thick central BHs, which might be responsible for the mid-IR excess. The 24 μm photometry is therefore still extremely valuable also in the case of bright 24 μm galaxies at $z = 2$, as it allows us to investigate this previously unidentified population of distant AGNs, relevant for the history of accretion onto supermassive BHs and their feedback on galaxy formation and evolution at a crucial epoch of massive galaxy formation.

The paper is organized as follows: In § 2 we describe the mid-IR excess galaxy sample and summarize all relevant background work described in full detail in the companion paper (Paper I). In § 3 we compare the mid-IR to UV estimated SFRs (i.e., the mid-IR excess) to a number of other observed galaxy properties and show that a warm dust component in addition to the colder star formation component is present in these galaxies at near-IR to mid-IR rest-frame wavelengths. The X-ray stacking analysis, unveiling the presence of heavily obscured AGNs, is presented in § 4, with the constraints on the absorbing gas column density suggesting that these sources are typically Compton-thick. We discuss the implications of these results with regard to the obscured AGN fraction at high redshifts, the X-ray background, the coeval growth of BHs and galaxies, and the AGN duty cycle in § 5; the possible relevance of these results for AGN feedback is discussed in § 6. Future prospects for further developments in understanding this previously unknown population of $z \sim 2$ AGNs are given in § 7. Summary and conclusions are provided in § 8. We quote stellar masses and SFRs for the case of a Salpeter initial mass function (IMF) from 0.1 and 100 $M_\odot$, and we adopt a *WMAP* cosmology with Ω_Λ, $\Omega_M = 0.74$, 0.26 and $h = H_0$(km s^{-1} Mpc^{-1})/100 = 0.73 (Spergel et al. 2007). Unless explicitly stated otherwise, we quote magnitudes in the Vega scale.

2. THE SAMPLE

2.1. *Galaxy Selection and Data Sets*

The data set and galaxy samples used in this paper are fully described in Paper I. For completeness we provide the relevant information here. We have selected sources in the K band to completeness limits of $K = 20.5$ in the GOODS-N and $K = 22$ in the GOODS-S field and then used the *BzK* color selection technique of Daddi et al. (2004a) to identify a total of ~1200 galaxies at $1.4 \lesssim z \lesssim 2.5$. Accurate photometric redshifts ($\sigma_z \sim 0.25$) and a large number of spectroscopic redshifts have been used. We exclude from the analysis the small fraction of contaminant *BzK* galaxies with $z < 1.2$ or $z > 3$. Sources of spectroscopic redshifts are described in Paper I and include all available public data sets, plus currently unpublished redshifts from the ultradeep (15–30 hr per mask) spectroscopy of the Galaxy Mass Assembly ultradeep Spectroscopic Survey (GMASS; J. Kurk et al. 2008, in preparation). We have excluded AGN-hosting galaxies by eliminating from the sample (1) sources with a 2–8 keV band detection in the 1 and 2 Ms Chandra Deep Field X-ray catalogs of Alexander

et al. (2003b) for GOODS-S and GOODS-N, respectively, and (2) sources with power-law SEDs over *Spitzer* IRAC and MIPS, lacking a distinct decrease in the flux density (f_ν) at wavelengths beyond 1.6 μm rest frame, based on visual classification (eventually, this removes only six galaxies in total due to power-law SEDs that were not also detected in the hard X-ray band). We also excluded 10% of the galaxies in the sample because of source blending due to the low resolution ($\sim 1.6''$) at IRAC wavelengths, which generally hampers measurement of accurate *Spitzer* MIPS 24 μm flux densities as well.

The main aim of Paper I is to investigate the nature of star formation at high redshift and to identify the best means to estimate the ongoing SFR activity. The work thus mostly focuses on *BzK star-forming* galaxies (as opposed to *BzK passive* galaxies). All the multiwavelength SFR indicators available in GOODS have been used. These include (1) the deepest current *Spitzer* MIPS 24 μm imaging (R. Chary et al. 2008, in preparation), reaching about 12 μJy (3 σ) in both fields; (2) the deepest current *Spitzer* MIPS 70 μm imaging, reaching about 1.8 mJy in part of both GOODS fields (Frayer et al. 2006; D. T. Frayer 2008, in preparation); (3) 160 hr of VLA[17] 1.4 GHz data in GOODS-N with 4.7 μJy of rms per beam (G. Morrison et al. 2008, in preparation); (4) 0.5–2 keV X-ray imaging from *Chandra* (used mainly in this paper, where we also discuss the AGN contamination that is needed for the interpretation of those data); (5) a deep 850 μm map of GOODS-N (Pope et al. 2005); and (6) UV photometry from GOODS ground-based and *Hubble Space Telescope* imaging (Giavalisco et al. 2004). The way in which photometry at these various wavelengths is interpreted to measure SFR in galaxies and the implied known limitations are described in § 3 of Paper I. The main results of Paper I, relevant to this work, are presented in §§ 4 and 5 of that paper. In summary, we find that a fraction of the $z = 2$ galaxies (generally those with the brightest mid-IR luminosities) have significant excess flux density in the mid-IR at 24 μm, i.e., at rest-frame ~ 8 μm, compared to the flux density expected on the basis of their ongoing star formation activity. A consistent mid-IR excess is also inferred from a comparison with radio, 70 μm, UV, and submillimeter (Paper I) (and soft X-ray, as discussed later in this paper) derived SFRs. We also find that the SFRs estimated from the dust reddening–corrected UV luminosities compare fairly well with respect to all other available indicators.

The aim of this paper is therefore to carefully identify and study the population of sources with mid-IR excess. In order to work with meaningfully defined galaxy samples, being able to compute accurately SFRs from both mid-IR and the UV, we limited in the following the analysis to 24 μm–detected sources with well-defined UV slopes [i.e., those with an error in $(B - z)$ color less than 0.4 mag]. This is required in order to obtain reasonable estimates of dust-corrected UV SFR ($\mathrm{SFR_{UV,corr}}$), with a formal error in the reddening correction lower than a factor of ≈ 2.

We further excluded galaxies that appear to be quiescent or have only a low level of star formation activity. These sources are generally very red in the UV because of relatively old stellar populations affecting the colors, and not simply because of dust reddening. For such sources the dust extinction correction is expected to fail, leading to overestimated $\mathrm{SFR_{UV,corr}}$, so that the comparison of mid-IR based SFRs to UV ones is not feasible. Based on the Paper I finding of a tight correlation between SFR and stellar mass at redshift $z \sim 2$ (as well known now to exist from $z = 0$ to 1; Elbaz et al. 2007; Noeske et al. 2007), we excluded quiescent galaxies as those for which the specific star formation rate $\mathrm{SSFR_{mid\text{-}IR}} < \mathrm{SSFR^0_{mid\text{-}IR}}/3$, where $\mathrm{SSFR} \equiv \mathrm{SFR_{mid\text{-}IR}}/\mathrm{mass}$ and $\mathrm{SSFR^0_{mid\text{-}IR}}$ is the median for 24 μm–detected $z \sim 2$ galaxies in GOODS. This criterion also requires a 24 μm detection.

2.2. *Definition of Mid-IR Excess Sources*

Following the results from Paper I, we define here mid-IR excess sources as sources satisfying

$$\log\left(\mathrm{SFR_{mid\text{-}IR+UV}}/\mathrm{SFR_{UV,corr}}\right) > 0.5. \quad (1)$$

Here $\mathrm{SFR_{mid\text{-}IR+UV}}$ is derived from the 24 μm flux density at the measured spectroscopic or photometric redshift and using the Chary & Elbaz (2001) templates, which are based on local mid- to far-IR correlations, with the addition of SFR estimated from the directly observed UV luminosity (nonreprocessed light from star formation). The term $\mathrm{SFR_{UV,corr}}$ is estimated from the UV after correcting for dust extinction based on the Calzetti et al. (2000) law (the average correction is a factor of ~ 40 for $K < 20$ sources [Daddi et al. 2005b] and decreases to a factor of a few to the faintest $K = 22$ limits). A galaxy can satisfy this mid-IR excess criterion either from overestimating the $\mathrm{SFR_{mid\text{-}IR}}$ with respect to $\mathrm{SFR_{UV}}$ or from underestimating the latter relative to the former. The first case corresponds to a genuine excess flux density in the mid-IR; the second one can be due to dust obscuration exceeding the Calzetti law prediction (optically thick UV emission). In Paper I it is shown that the second case is relevant at most for a small fraction of the sample ($\lesssim 15\%$), and therefore the vast majority (but not all) of mid-IR excess sources are overluminous, for some reason, at mid-IR wavelengths.

It is important to recall here that the luminosity-dependent Chary & Elbaz (2001) templates that we adopt have been built on the basis of the local correlations in the mid-IR to far-IR for star-forming galaxies. A mid-IR excess with respect to these SEDs is equivalent to a mid-IR excess with respect to the SED of standard star-forming galaxies in the local universe. In any case, it should be clarified that this population of mid-IR excess galaxies is well defined independently of the class of SEDs used to interpret the mid-IR luminosities. As shown extensively in Paper I, $z = 2$ galaxies at a given intrinsic SFR or bolometric luminosity appear to display a wide range in their $L(8\ \mu\mathrm{m})$. Therefore, mid-IR excess galaxies can be also seen as galaxies with $L(8\ \mu\mathrm{m})$ larger than the average $\langle L(8\ \mu\mathrm{m})\rangle$ of galaxies of a given SFR (or of local star-forming galaxies with the same SFR). Deviations from the normal $L(8\ \mu\mathrm{m})$ versus SFR relation are also observed in the local universe and generally ascribed to the presence of an AGN (e.g., Genzel et al. 1998; Laurent et al. 2000; Dale et al. 2006; Armus et al. 2007).

The threshold chosen in equation (1) (0.5 dex, about a factor of 3) is dictated by the evidence that, in the opposite direction to mid-IR excess galaxies, there are very few galaxies with $\mathrm{SFR_{UV,corr}}$ in excess of more than a factor of 3 of $\mathrm{SFR_{mid\text{-}IR+UV}}$ (Fig. 1). This suggests that samples of genuinely discrepant galaxies with too high ratios are to be found above a similar threshold, assuming that intrinsic scatter in the ratio is to first order symmetrical.[18] We later show that this threshold is well defined also with respect to the X-ray properties of the samples.

Although the use of UV as the primary SFR indicator is less than optimal because of the possibility for substantial obscuration from thick lines of sight, it is the only one available for nearly all

[17] The National Radio Astronomy Observatory is a facility of the National Science Foundation operated under cooperative agreement by Associated Universities, Inc.

[18] It is worthwhile to emphasize that, despite the large dust reddening corrections to $\mathrm{SFR_{UV,corr}}$, most sources in Fig. 1 cluster around a ratio of 1, and the Gaussian component in the distribution has a dispersion of only ~ 0.2 dex.

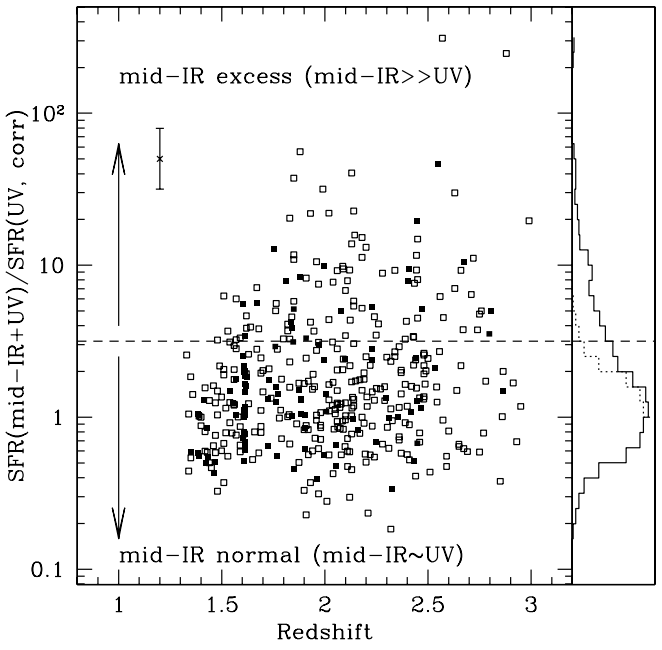

FIG. 1.—Ratio of mid-IR–based to UV-based SFR plotted as a function of the redshift. Here and in several of the figures in this paper, we plot only the GOODS-S portion of the galaxy sample, being deeper and extending to $K < 22$. Filled squares indicate spectroscopic redshifts, while open squares indicate photometric redshifts. The horizontal line defines the separation between mid-IR excess and normal galaxies, as given by eq. (1). The rightmost panel shows the distribution of sources as a function of mid-IR excess ratio. The dotted line is the reflection of the bottom part of the histogram around a ratio of 1. The error bar in the top left part of the figure shows the typical error in the SFR ratio, inferred from the spread of the histogram around a ratio of 1. [*See the electronic edition of the Journal for a color version of this figure*.]

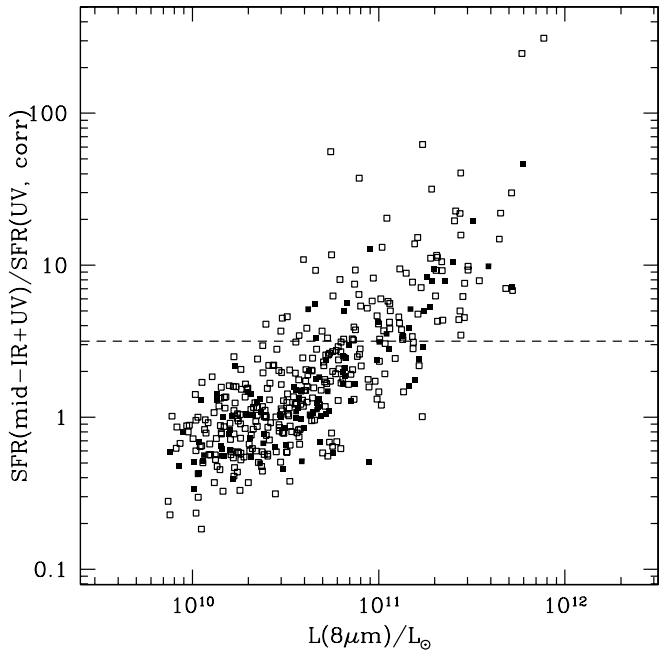

FIG. 2.—Mid-IR excess is observed to correlate with the mid-IR luminosity of galaxies (Paper I; the lack of sources in the top left part of the plot might be in part a selection effect). Symbols are as in Fig. 1. The majority of the sources with $L(8\ \mu\mathrm{m}) > 10^{11}\ L_{\odot}$ would be classified as mid-IR excess sources based on the definition in eq. (1). Multiwavelength analysis in Paper I (and later in this paper) shows that the excess is present with respect to radio, UV, 70 μm, soft X-ray, and submillimeter SFR indicators. [*See the electronic edition of the Journal for a color version of this figure*.]

24 μm sources at $z \sim 2$ in GOODS (the other SFR indicators being limited by sensitivity and applicable individually to only a fraction of the galaxies, e.g., 20% for radio).

The combination of the requirements discussed in the previous section leaves us with a total sample of 430 (183) galaxies in the GOODS-S (GOODS-N) field, or about 50% of the primary sample. Of these, 106 (58) satisfy equation (1) and are therefore classified as mid-IR excess galaxies, representing 24.6% (31.7%) of the total sample. Likewise, robust spectroscopic redshifts are available for 108 (44) galaxies, or 25.1% (24.0%) of the total sample. Most of the mid-IR excess sources have very high 8 μm rest-frame luminosities, often in excess of $10^{11}\ L_{\odot}$ (Fig. 2), and the vast majority of galaxies in our sample having $L(8\ \mu\mathrm{m}) > 10^{11}\ L_{\odot}$ also show a mid-IR excess. This is reminiscent of finding that most luminous IR galaxies in the local universe tend to be AGN dominated (e.g., Tran et al. 2001).

3. MID-IR EXCESS AND OTHER GALAXY PROPERTIES

With the aim of understanding the nature of the sources with mid-IR excess and therefore the origin of this excess, we have searched for the existence of possible correlations of this excess with other galaxy properties.

3.1. *UV Slopes, Redshift, Morphology, and Colors*

As shown in Figure 13 of Paper I, the mid-IR excess does not strongly depend on the UV slope of the galaxies, and we therefore exclude that it is due to effects inherent in the correction for reddening of the UV luminosity. A possible origin of the excess could instead be mid-IR SED evolution with redshift, within the $1.2 < z < 3$ range populated by our sample. We have checked if mid-IR excess sources preferentially appear at some high or low redshift within the $z \sim 2$ sample (Fig. 1). There is a tendency for $z \sim 1.5$ sources to have low mid-IR to UV ratios. This could be due to 9.7 μm silicate absorption entering the 24 μm *Spitzer* MIPS bandpass, or to an overestimation of the reddening correction at these lowest redshifts. There is also a tendency for sources with the strongest excess to be located at $z \gtrsim 2$. However, the median ratio of mid-IR– to UV-based SFRs is fairly stable as a function of redshift, and no strong trend with redshift is detected. If we are seeing galaxies with anomalous mid-IR SEDs, compared to $z \sim 0$, they are rather homogeneously distributed in the probed redshift range.

We have performed Sérsic index fitting using Galfit (Peng et al. 2002) to the ACS F850W band images of our sample of $z = 2$ galaxies in GOODS-S. Results and full details will be presented in S. Ravindranath et al. (2008, in preparation). Comparing the Sérsic index and size distributions of mid-IR excess and normal galaxies, we do not find statistically significant differences for the full sample with $K < 22$ in GOODS-S.

Instead, we find a strong correlation of the mid-IR excess with the (K − IRAC) colors. Figure 3 shows that mid-IR excess objects have redder ($K - 5.8$ μm) colors. Galaxies with spectroscopic redshift follow the same trend of those with only a photometric redshift. Similar trends are observed for the other three IRAC channels (3.6, 4.5, and 8.0 μm, not shown here). In principle, redder colors could suggest higher than average redshifts due to K-correction effects, but this is ruled out by the weak trend with redshift that we observe, e.g., for the ($K - 5.8$ μm) color. We conclude that the optical to near-IR rest-frame colors of mid-IR excess sources are intrinsically redder than those of normal sources. These results imply that whatever the cause of 24 μm flux density excess in these galaxies, this excess is detectable also toward shorter wavelengths as seen in the IRAC bands. The distribution in the SFR ratio shown in Figure 3 for $K - 5.8$ μm < 1 colors

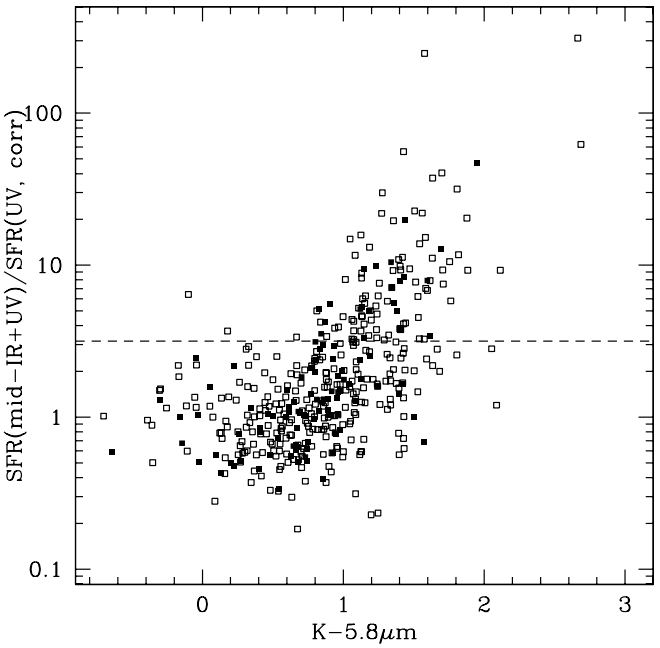

FIG. 3.—Ratio of mid-IR– to UV-based SFR plotted as a function of the ($K - 5.8$ μm) color, in the AB scale, for the GOODS-S field. Symbols are as in Fig. 1. The figure shows that mid-IR excess sources are systematically redder in $K - 5.8$ μm color than normal galaxies. [*See the electronic edition of the Journal for a color version of this figure.*]

supports our choice of the factor of ~3 ratio in equation (1) for defining mid-IR excess sources.

3.2. *Median SEDs of Galaxies with and without Mid-IR Excess*

The systematic difference observed for colors reflects different typical SEDs between the UV/optical and the near-IR rest frame. We have derived multiwavelength rest-frame SEDs of mid-IR excess and normal galaxies by computing the median magnitude for galaxies in each sample. Results are shown in Figure 4 for GOODS-N and GOODS-S. This visually confirms that excess emission is detected at all rest-frame wavelengths greater than 1 μm. The typical $SFR_{UV,corr}$ of the two samples are very close for GOODS-N, as can be inferred from the similarity of the SEDs below 1 μm [implying also similar median $E(B - V)$]. Being much deeper in K band, the GOODS-S mid-IR normal sample has lower $SFR_{UV,corr}$ than the mid-IR excess sample by some 25%–30%. Mid-IR excess sources tend to be found more often at brighter K magnitudes, as one can argue from the figure (see also the next section). This explains the larger difference in the normalization of the SEDs above 1 μm rest frame. At the shortest wavelengths probed here, it is instead the normal galaxies that have brighter median magnitudes. This is due to the fact that fainter galaxies are bluer (see, e.g., also Daddi et al. 2004a).

More importantly, we notice that the peak of the stellar-dominated component of the SED (say, below 2–3 μm rest frame) of mid-IR excess objects is located at longer wavelengths than in normal galaxies (e.g., IRAC 5.8 μm band vs. 4.5 μm band), where the peak is consistently located at ~1.6 μm as expected (e.g., Sawicki 2002). This difference persists when accounting for the slightly higher redshifts of mid-IR excess objects ($z \sim 2.1$ vs. $z \sim 1.9$ on average). In order for this difference to vanish, one might assume that mid-IR excess objects are at even higher redshifts than inferred here. In turn, the mid-IR excess would vanish if we assume that these galaxies are actually systematically at lower redshifts than estimated here (which would increase more strongly $SFR_{mid\text{-}IR+UV}$ than $SFR_{UV,corr}$). However, there is no way to eliminate both the mid-IR rest-frame excess and near-IR rest-frame excess by simply moving the SEDs in redshift.[19] This is an

[19] If these were otherwise normal galaxies (also in their mid-IR) with just photometric redshifts (and thus $SFR_{mid\text{-}IR+UV}$) largely overestimated, we should have found the peak of the stellar SEDs at lower rest-frame wavelengths than in normal galaxies. If we had instead underestimated the redshifts of the sources (but notice that objects with z_{spec} and z_{phot} behave consistently in Fig. 3), placing them at even higher redshifts would further increase the strength of the excess seen at 24 μm.

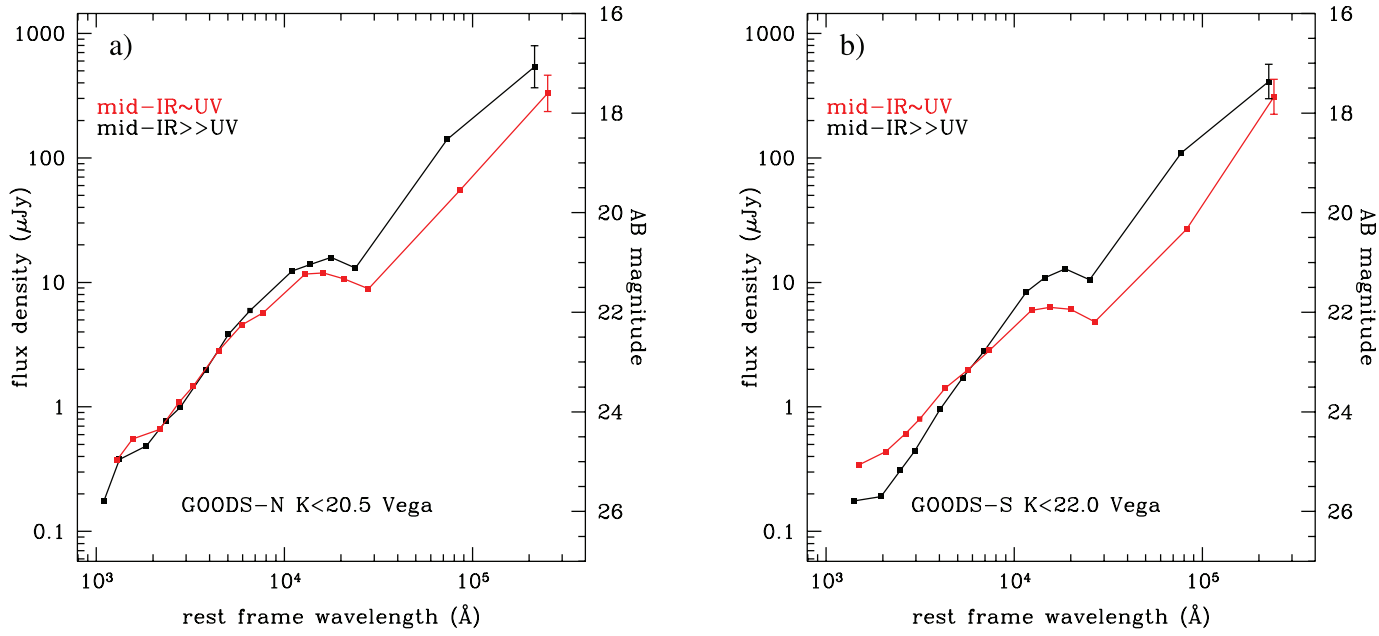

FIG. 4.—Median SEDs of mid-IR excess objects (*black*) compared to those of galaxies with more normal mid-IR properties (*red*). (*a*) GOODS-N field, limited to $K < 20.5$; (*b*) GOODS-S, to $K < 22$. The GOODS-S photometry includes *BVIzJHK*, the four *Spitzer* IRAC bands, and *Spitzer* MIPS 24 and 70 μm. In GOODS-N we have the same, plus U band.

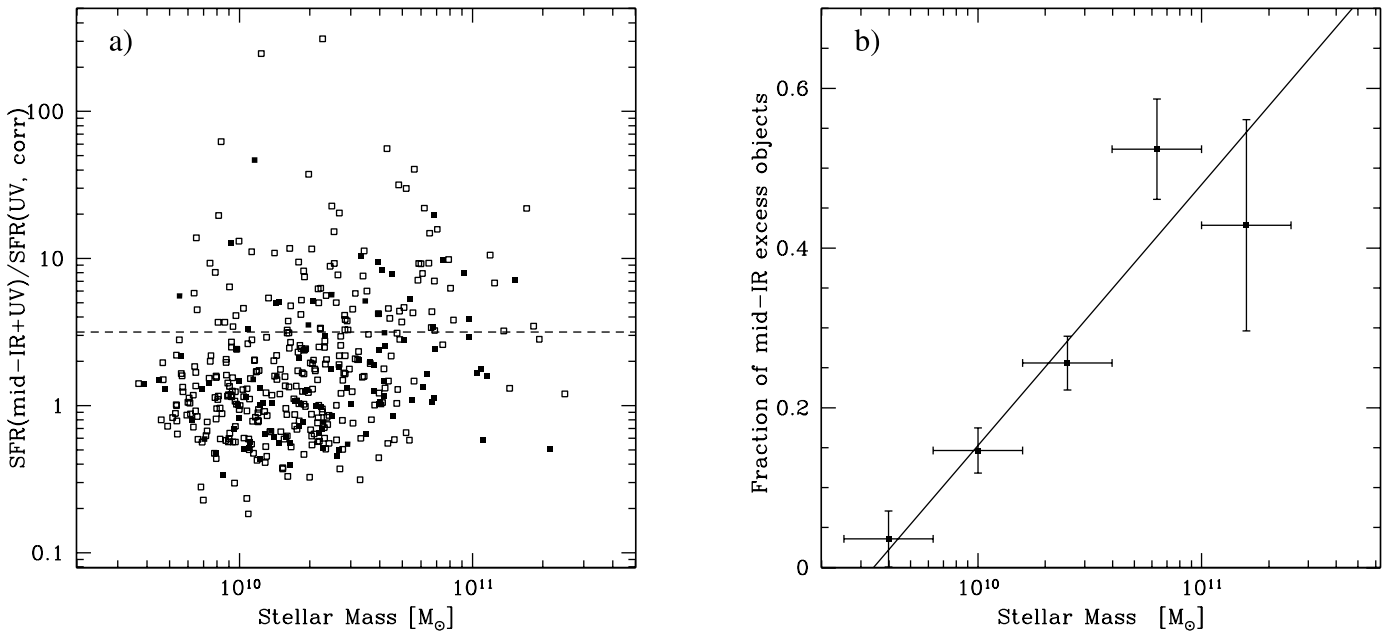

FIG. 5.—(*a*) Ratio of mid-IR– vs. UV-inferred SFR plotted against stellar mass. Symbols are as in Fig. 1. (*b*) Fraction of mid-IR excess objects inside star-forming galaxies as a function of stellar mass. Bins are spaced by 0.4 dex and contain sources within ±0.2 dex in stellar mass (i.e., the 5 bins plotted are independent). The line is a weighted linear fit to the data. Error bars on the fractions are Poisson, while error bars in the *x*-axis reflect the width of the bin. [*See the electronic edition of the Journal for a color version of this figure.*]

important piece of evidence demonstrating that we are finding mid-IR excess galaxies not simply as the result of biases in the photometric redshifts.

In principle, an SED peak longward of 1.6 μm could be due to extremely strong dust reddening (e.g., Chary et al. 2007). However, this is disfavored by the comparison of the UV slopes and further by the agreement between the radio and UV SFRs, which rules out substantial additional obscuration in the UV (beyond the obscuration that we estimate based on the UV slopes). We also tested that these results are robust if restricted to sources with spectroscopic redshifts only, and if excluding (in GOODS-N) sources that are radio detected and could be truly UV obscured cases. We conclude that from the SEDs there is compelling evidence that the mid-IR excess is intrinsic and extends to near-IR rest-frame wavelengths, in such a way that the SED shape is altered and its peak moved to wavelengths longer than 1.6 μm (to about 1.8–1.9 μm). The required excess component increases sharply with wavelength up to $\sim$10 μm rest frame.

Stacking of sources at 70 μm (after excluding the few individual detections) yields $\gtrsim$3 σ detections for both mid-IR excess and normal galaxies in both GOODS-N and GOODS-S fields (Fig. 4). In both fields, mid-IR excess and normal galaxies have 70 μm stacked flux densities in agreement within the errors, although in both fields the mid-IR excess sources are marginally brighter (less than 1 σ significance in both cases). This is consistent with the two classes having comparable underlying SFRs. This also implies that the excess emission is getting less important, in relative terms, when sampling $\sim$20 μm rest-frame wavelengths with the 70 μm imaging. The observed 70 μm–to–24 μm ratio is 3.2 and 3 for mid-IR excess galaxies in GOODS-N and GOODS-S, respectively, less than half the ratio expected for a local ultraluminous infrared galaxy (ULIRG) if placed at $z \sim 2.1$. The ratios for the normal galaxies are in better agreement with those expected from the Chary & Elbaz (2001) models based on local correlations. This trend is similar to that found by Papovich et al. (2007).

The mid-IR excess therefore manifests itself as a relatively warmer continuum dust emission, with respect to the star formation components, whose contribution peaks in the mid-IR but is still detectable in the near-IR rest frame. This kind of warm emission is unlikely to be star formation dominated, as the reprocessed emission from star formation declines very steeply below 5 μm (Genzel et al. 1998; Laurent et al. 2000), and is a clear signature of the presence of an AGN. These galaxies could be similar to those selected as putative AGN hosts on the basis of power-law continua over the same wavelength range (e.g., Alonso-Herrero et al. 2006; Donley et al. 2007), but with a smaller relative contribution of the AGN at least in the IRAC bands, at near-IR rest-frame wavelengths. By comparing the excess at near-IR and mid-IR rest-frame wavelengths, we find that the additional contribution has a shape comprised between that of the nucleus of NGC 1068 and of Mrk 231 (at a fixed 24 μm excess, NGC 1068 underpredicts and Mrk 231 overpredicts the median excess over the IRAC bands).

This contamination observed in the IRAC bands will have consequences for SED fitting with stellar population models to derive stellar population parameters and stellar masses. We explore this issue in more detail in C. Maraston et al. (2008, in preparation). This contamination can also affect the estimation of photometric redshifts of $z \sim 2$ galaxies when using IRAC bands, as this estimate relies also on the location of the 1.6 μm bump of the stellar SEDs. Comparing to our set of spectroscopic redshifts, we can in fact detect a small bias, with the photometric redshifts of mid-IR excess galaxies being slightly overestimated. Compared to normal galaxies, the median difference between photometric and spectroscopic redshifts is larger by about 0.04 (0.09) in GOODS-S (GOODS-N), just a few percent of $(1 + z)$.

It is also important to recall here that the warm continuum contamination of the SEDs disappears, or at least is entirely negligible, over the UV rest frame. This is based on the median SEDs shown and also on the consistency of UV-based SFR estimates and submillimeter, radio, and 70 μm, for both mid-IR excess and

normal galaxies, as extensively discussed in Paper I. In addition, no AGN emission lines are generally detectable in the UV from the mid-IR excess objects, even in the ultradeep 15–30 hr integration GMASS spectroscopy. This is also consistent with the result that the rest-frame UV morphological properties of mid-IR excess and normal galaxies are similar.

3.3. *Mid-IR Excess and Stellar Mass*

We have checked if and how the incidence of mid-IR excess galaxies varies with the inferred stellar mass (Fig. 5). Stellar masses for our sample are estimated from the empirically calibrated relations presented in Daddi et al. (2004a), as discussed in Paper I, based on the observed photometry in the B, z, and K bands. We find that mid-IR excess sources tend to preferentially reside in galaxies with larger than average stellar masses. The fraction of mid-IR excess sources increases steeply with the mass of the galaxies.

We have investigated if the relation shown in Figure 5 could be the result of a selection effect. First, we have checked that the trend formally remains if we add to the sample the galaxies with uncertain measurements of the UV slope (and therefore of the UV SFR and mid-IR excess). Also, the sample plotted in Figure 5 is not mass complete to the lowest masses it formally reaches ($\sim 0.5 \times 10^{10}\ M_{\odot}$). Given our K-band selection to $K < 22$ (for the GOODS-S sample shown in the figure on which this analysis is based), we expect to be largely complete only above $\sim(2-3) \times 10^{10}\ M_{\odot}$. We would miss star-forming galaxies below this stellar mass threshold if they have very red colors. However, we have verified that we still find statistical evidence for an increasing fraction of mid-IR excess sources with stellar mass if we limit the sample to the range in stellar masses that is expected to be highly complete. Similarly, if we limit our analysis to blue galaxies only, for which we are mass complete over nearly the whole mass range, we still recover the trend shown in Figure 5.

The *warm continuum* contribution detected over the IRAC bands is unlikely to bias the results on the dependence of the fraction of mid-IR excess galaxies with stellar mass. Already over the IRAC bands the typical excess contribution is less than 0.5 mag,[20] and we recall that the stellar mass estimates are not derived using the IRAC bands, but only up to K band. The presence of a few tenths of magnitudes of AGN contribution in the observed K band would not alter substantially the trend. Therefore, we conclude that this result is solid and not simply a selection bias.

In Paper I we describe a strong correlation between stellar mass and $\mathrm{SFR_{UV,corr}}$. Because of this correlation, the fraction of mid-IR excess objects also increases with $\mathrm{SFR_{UV,corr}}$. This effect is less pronounced and less evident than the one found for the stellar mass.

4. X-RAY PROPERTIES

The overall properties of mid-IR excess sources, as explored in the previous sections, point to the presence of a warm mid-IR continuum component, which could be due to AGN activity. Since we have removed from the sample all X-ray–identified AGNs in the 2–8 keV band, any powerful ($L_{\mathrm{X}} \gtrsim 10^{43}$ ergs s^{-1}) AGN present in the mid-IR excess objects would have to be heavily obscured in order to escape being individually detected in the X-rays (note that the observed 2–8 keV band corresponds to the rest-frame 6–24 keV band). We can search for the signature of heavily obscured AGNs below the X-ray detection limit using X-ray stacking analyses (e.g., Brandt et al. 2001). Here we use the code adopted by Worsley et al. (2005), which stacks sources and calculates the significance of the stacked result using 10,000 Monte Carlo trials. In all cases, we limit the X-ray stacking to sources within 5.5′ of the *Chandra* aim point, to maximize sensitivity.

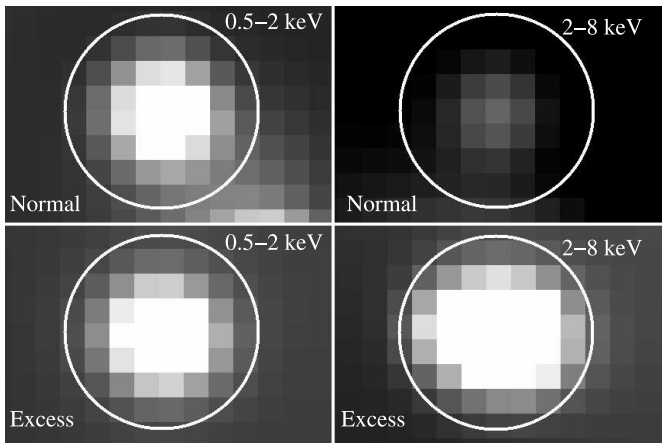

FIG. 6.—Soft and hard X-ray *Chandra* stacked images of normal and mid-IR excess $z = 2$ objects in GOODS-S. Left panels show the soft (0.5–2 keV) bands, while the right panels are for hard (2–8 keV) bands. The top two images are for normal galaxies, while the bottom two are mid-IR excess objects. It is evident that similar soft X-ray fluxes are detected in the two samples, but much stronger hard emission is detected for the mid-IR excess $z \sim 2$ galaxies. Images have been smoothed by a Gaussian with the size of the point-spread function. The circles (4″ diameter) show the expected location of the signal.

4.1. *X-Ray Stacking Results*

We stacked 59 mid-IR excess galaxies in GOODS-S and found a 5 σ detection in the 2–8 keV band and an 8 σ detection in the 0.5–2 keV band (Fig. 6). The count ratio (H/S) is 0.90 ± 0.13, corresponding to a nominal power-law photon index $\Gamma = 0.8^{+0.4}_{-0.3}$. Using $\Gamma = 0.8$, we infer an average 2–8 keV flux of 5.6×10^{-17} ergs s^{-1} cm^{-2} and an average 0.5–2 keV flux of 1.1×10^{-17} ergs s^{-1} cm^{-2}. The flat X-ray spectral slope strongly argues for the presence of heavily obscured AGNs (see, e.g., Fig. 2 of Alexander et al. 2005a). The 175 *normal* GOODS-S sources (i.e., those without mid-IR excess) give a stacked 3 σ signal in the 2–8 keV band and a 12 σ detection in the 0.5–2 keV band (Fig. 6). The band ratio is 0.36, corresponding to a spectral index $\Gamma \sim 1.7$, which is fully consistent with star formation dominating the X-ray emission (e.g., Persic & Rephaeli 2002). Using this value of Γ, we derive a 2–8 keV flux of 1.6×10^{-17} ergs s^{-1} cm^{-2} and a 0.5–2 keV flux of 1.0×10^{-17} ergs s^{-1} cm^{-2}. Stacking analysis of the smaller GOODS-N sample, which is limited to $K < 20.5$, gives a slightly less secure detection and lower signal-to-noise ratios (S/Ns), although still with hard X-ray fluxes twice as large for mid-IR excess versus normal galaxies. Similar properties are seen in the GOODS-S sample when limited to $K < 20.5$. In the following we concentrate on the GOODS-S sample to $K < 22$ because it has the highest S/N X-ray detections. The results of the X-ray stacking are listed in Table 1.

The observed X-ray fluxes can be directly used to estimate luminosities, without accounting for obscuration. For the mid-IR normal galaxies in the GOODS-S sample ($\langle z \rangle = 1.9$), we infer isotropic luminosities of 2.7×10^{41} ergs s^{-1} in the 2–8 keV rest-frame band (mapping very closely to the 0.5–2 keV observed band) and 4.2×10^{41} ergs s^{-1} in the 5.8–23.2 keV rest-frame band, assuming a $\Gamma = 1.9$ spectral slope. For mid-IR excess galaxies in

[20] This is true for both GOODS fields; we recall that the larger difference in the SED normalizations over the IRAC bands that is observed in GOODS-S is mainly due to the different median stellar mass between mid-IR excess and normal galaxies (Fig. 5).

TABLE 1
X-Ray Stacking Analysis of GOODS $z = 2$ Galaxies

Sample	N	Exp SB (Ms)	Counts (10^{-6} s^{-1}) FB	SB	HB	S/N FB	SB	HB	Flux (10^{-17} cgs) FB	SB	HB
Normal											
$K < 20.5$ N	69	121.2	2.05	1.42	0.65	6.6	8.4	2.4	1.78	0.74	1.32
$K < 20.5$ S	58	49.3	3.33	2.35	1.01	6.8	8.4	2.5	2.94	1.25	2.24
$K < 22.0$ S	175	146.7	2.52	1.86	0.68	9.0	11.7	2.9	2.23	0.99	1.50
Excess											
$K < 20.5$ N	27	47.2	3.80	2.57	1.26	7.3	9.0	2.8	3.29	1.35	2.55
$K < 20.5$ S	27	22.8	4.09	2.88	1.24	6.0	7.5	2.2	3.61	1.53	2.76
$K < 22.0$ S	59	49.8	4.01	2.13	1.92	8.6	8.0	5.0	6.84	1.07	5.62[a]

Notes.—N is the number of sources that were stacked. FB is full band (0.5–8 keV), SB is soft band (0.5–2 keV), and HB is hard band (2–8 keV). A total of 10,000 Monte Carlo trials are performed to estimate the background and S/N for each sample. Effective exposure time is measured in the soft band. Fluxes are calculated using the X-ray spectral slope of $\Gamma = 0.8$ for the $K < 22$ GOODS-S mid-IR excess galaxies and assuming $\Gamma = 1.9$ for the samples that are not detected in the hard band.

[a] Using the model shown in Fig. 9, we derive a $\sim$1.7 times higher flux of 9.55×10^{-17} ergs s^{-1}.

GOODS-S ($\langle z \rangle = 2.1$), the fluxes correspond to X-ray luminosities of 3.8×10^{41} ergs s^{-1} in the 2–8 keV rest-frame band and 2×10^{42} ergs s^{-1} in the 6.2–24.8 keV rest-frame band, for the spectral slope of $\Gamma = 0.8$ derived from the count ratios.

We have explored how these X-ray stacking results depend on the threshold of 0.5 dex in the ratio of $SFR_{mid\text{-}IR+UV}$ to $SFR_{UV,corr}$ that we have adopted in equation (1) for defining mid-IR excess sources. We have varied the threshold from 0.2 to 1.0 dex and performed X-ray stacking separately for sources above and below the threshold. Figure 7 shows that the general X-ray properties of the "normal" populations are quite insensitive to the threshold at which the *excess* sources are identified, given that the latter ones are in all cases a minority. For the mid-IR excess sources, the X-ray stacking confirms that a threshold 2–5 in the SFR ratio effectively singles out the population of hard X-ray emitters (with similar count rates in both hard and soft *Chandra* bands). The X-ray count rates, and therefore the average luminosities of the mid-IR excess sources, increase with the threshold, while their space density obviously decreases, but the accuracy in the measurements declines due to lower number statistics.

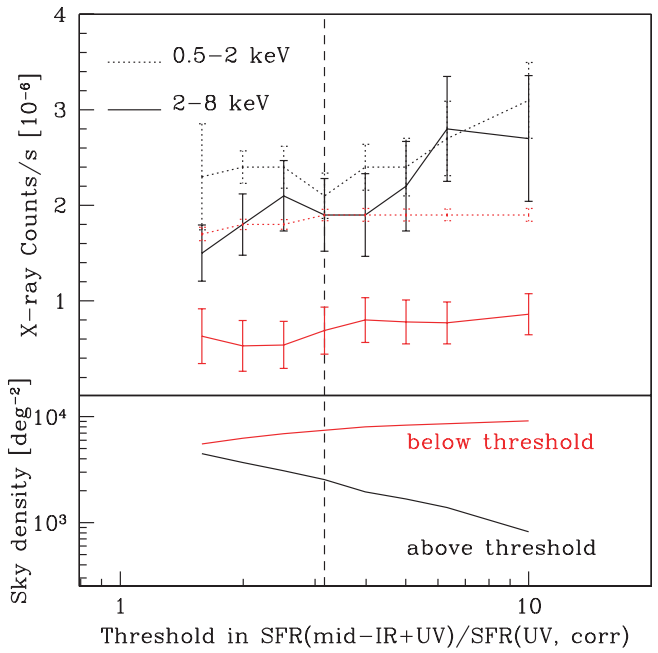

Fig. 7.—*Top*: X-ray counts from stacking of mid-IR excess vs. mid-IR normal sources for a variety of thresholds separating these two classes: from 0.2 to 1.0 dex in the ratio of $SFR_{mid\text{-}IR+UV}/SFR_{UV,corr}$. Black lines are for mid-IR excess sources (with ratio above the threshold), while red lines are for mid-IR normal sources (with ratio below the threshold). Solid lines show hard (2–8 keV band) counts, while dotted lines show soft (0.5–2 keV band) counts, from stacking *Chandra* data in the 1 Ms GOODS-S field. *Bottom*: Sky density of the two populations, as a function of the defining threshold. We are not applying here completeness corrections to the sample (see § 5.1).

A possible concern with stacking analyses is whether a small subset of bright sources dominate the stacked results. We verified that this is not the case by performing stacking in galaxy subsamples. The results shown in Figure 7 argue that our X-ray stacking conclusions are robust to the exact definition of the sample.

Although the X-ray band ratio indicates the presence of obscured AGNs, it does not fully characterize the properties of the sources. We can gain additional insight into the X-ray spectral properties of mid-IR excess sources by stacking the data inside narrower energy bands. Stacking the GOODS-S data using the sub-bands 0.5–2, 1–2, 2–4, 4–6, 4–8, and 6–8 keV, one obtains the results shown in Figures 8 and 9 and Table 2. Significant ($\gtrsim 3\,\sigma$) detections are found in all of the sub-bands, except for the 6–8 keV band where the detection is only at the 1.8 σ level (still noteworthy given the low sensitivity of *Chandra* at these high energies). In summary, the mid-IR excess sources exhibit a hard X-ray spectrum that becomes harder with increasing energy, an unequivocal signature of highly obscured AGN activity.

4.2. *X-Ray–inferred SFRs*

The soft X-ray (0.5–2 keV band) fluxes of the samples (mapping quite closely to the rest-frame 2–8 keV luminosities at $z = 2$) can be used to estimate SFRs, since for star-forming galaxies this is proportional to the population of massive X-ray binaries (Ranalli et al. 2003; Persic et al. 2004; Hornschemeier et al. 2005). The rest-frame 2–8 keV luminosity of mid-IR excess sources is $\sim$30% higher than that of mid-IR normal sources and would thus suggest $\sim$30% higher SFRs for the former. This is in excellent agreement with the estimate obtained from the UV, where we find the same offset between the average $SFR_{UV,corr}$ of the two samples and in

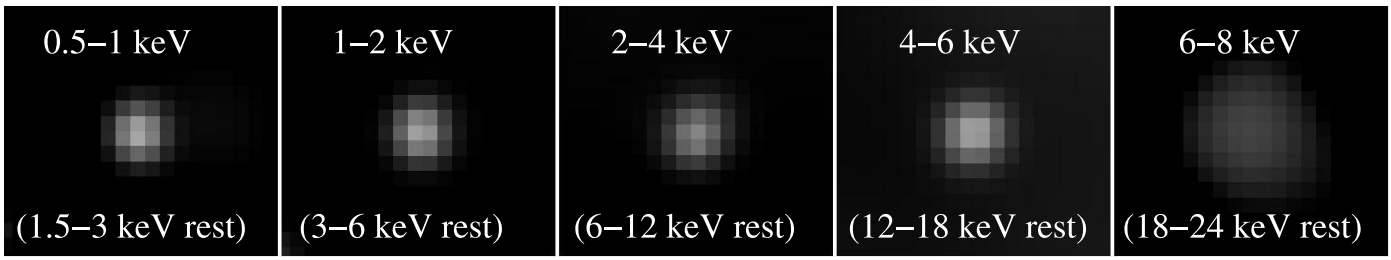

FIG. 8.—*Chandra* sub-band stacking detections of mid-IR excess $z \sim 2$ galaxies. The images have been smoothed with the point-spread function of the band, to enhance the signal visibility. Each panel size is 12″.

the same direction. Interestingly, the proportionality that we derive is

$$\mathrm{SFR}_{\mathrm{UV,corr}}\left(M_{\odot}\ \mathrm{yr}^{-1}\right) = 2.25 \times 10^{-40} L_{2-8\ \mathrm{keV}}\left(\mathrm{ergs\ s}^{-1}\right), \quad (2)$$

which is very close to the relation given in Ranalli et al. (2003) (the Persic et al. [2004] relation only accounts for the contribution of high-mass X-ray binaries). The agreement between the UV- and X-ray–estimated SFRs, for both samples of normal and mid-IR excess galaxies in GOODS-S, suggests that no substantial AGN contribution is detected in the observed 0.5–2 keV band of these mid-IR excess objects. Similarly, we find that the soft X-ray fluxes in the mid-IR excess samples in both fields, when limited to $K < 20.5$, are fully accounted for by the SFR inferred from UV.

4.3. *Evidence for Compton-thick AGNs*

Estimating the obscuring column density for the AGNs inside mid-IR excess sources is crucial for deriving their intrinsic properties. Their stacked *Chandra* 0.5–2 keV/2–8 keV band ratio implies an absorbing gas column density $N_{\mathrm{H}} \sim 10^{23.3}$ cm^{-2}, for an underlying standard AGN power-law continuum with $\Gamma = 1.9$. Therefore, these AGNs are clearly obscured, but this estimate of N_{H} should be regarded as a strict lower limit because star formation is contributing to the emission, especially in the soft band. The 0.5–2 keV emission of the mid-IR excess galaxies can be entirely ascribed to their ongoing star formation, as discussed in the previous section. If we consider that the AGN component in the 0.5–2 keV band is consistent with zero given the errors, we formally obtain a 2 σ lower limit $N_{\mathrm{H}} > 10^{23.9}$ cm^{-2} for an intrinsic AGN power-law continuum with $\Gamma = 1.9$.

We further used the result of spectral stacking shown in Table 2 and Figure 9 to improve our constraints on N_{H}. Figure 9*b* shows the X-ray spectrum at 2–20 keV rest-frame energies of the mid-IR excess sources, after subtraction of a star formation component (dashed line model shown in Fig. 9*a*). We have fitted this AGN component with the Gilli et al. (2007) models for obscured AGNs, where N_{H} is increased in steps of 1 dex up to $N_{\mathrm{H}} = 10^{25.5}$ cm^{-2}

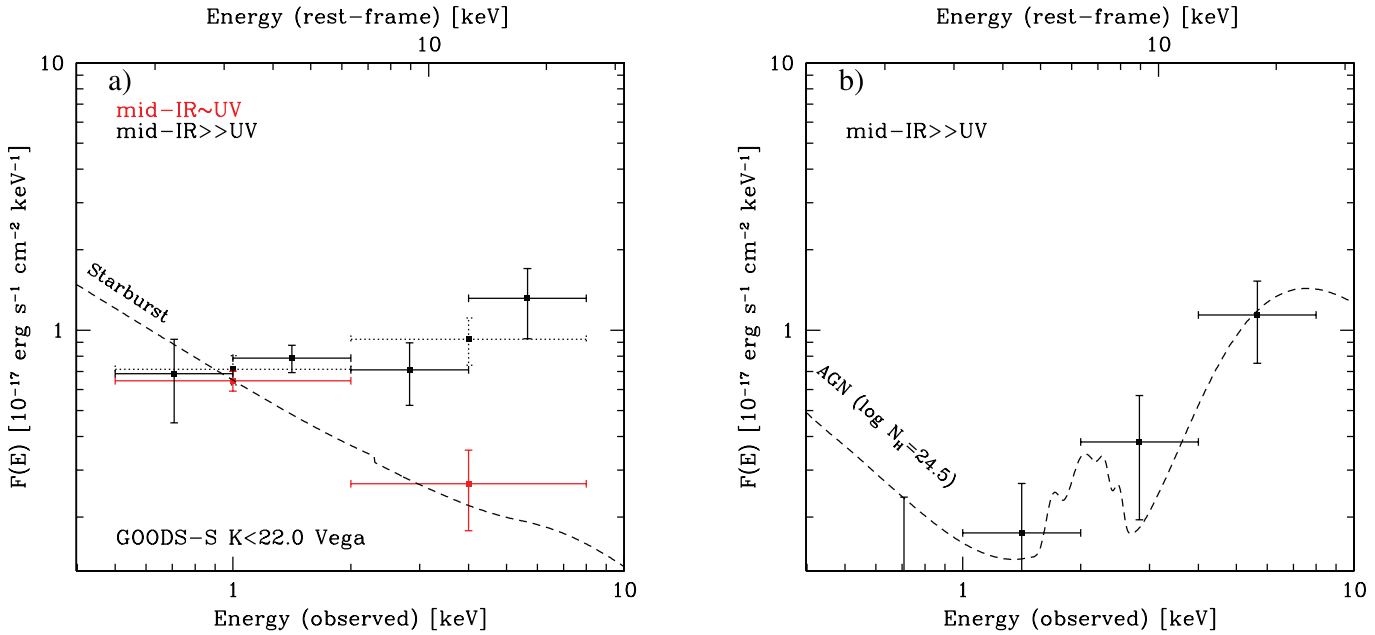

FIG. 9.—(*a*) X-ray measurements of flux per unit energy [$F(E)$] for mid-IR excess sources (*black*) and normal sources (*red*). It is evident that mid-IR excess sources are much harder, inconsistent with pure star formation as indicated by the photon index $\Gamma = 1.9$ power law (starburst). Sub-band stacking of mid-IR excess sources (*black points with solid error bars*) reveals that their $F(E)$ continue to rise at the highest energies. These sources are consistent with a combination of star formation plus a heavily obscured AGN component rising toward the highest energies. (*b*) Result of subtracting the SFR component from the sub-band *Chandra* stacking of the mid-IR excess galaxies, normalized to the soft-band point (allowing for a plausible range of uncertainty to this quantity does not substantially alter the results). The overplotted line is an AGN model with $N_{\mathrm{H}} = 10^{24.5}$ cm^{-2} (Gilli et al. 2007) convolved with the redshift distribution of the sample. The bump in the models near 2 keV (in the observed frame) is due to the strong Fe emission line expected to be prominent in obscured AGNs.

TABLE 2
STACKED X-RAY SPECTRA

Band	Counts (10^{-6} s^{-1})	S/N	Flux (10^{-17} cgs)
0.5–1 keV.....	0.57	2.9	0.34
1–2 keV.....	1.67	8.5	0.79
2–4 keV.....	0.89	3.8	1.42
4–8 keV.....	1.16	3.4	5.25
6–8 keV.....	0.47	1.8	4.94

NOTES.—Results of the X-ray spectral stacking for mid-IR excess objects in GOODS-S to $K < 22$. Fluxes are calculated using the overall X-ray spectral slope of $\Gamma = 0.8$, estimated from the X-ray band ratio. S/N of the data is calculated using the background estimated from 10,000 Monte Carlo trials.

(this approach is admittedly crude, but there is little point for a more refined approach in this work). At the highest levels of obscuration, beyond the Compton-thick regime of $N_{\rm H} = 10^{24}$ cm^{-2}, reflection components start to be important in the AGN emission in the rest-frame ~2–8 keV (observed *Chandra* 0.5–2 keV for $z \sim 2$), as well as the emission from the Fe Kα line at 6.4 keV, and both are properly included in the models of Gilli et al. (2007). Having convolved the templates with the observed redshift distribution of our sample, the best fit is obtained for $N_{\rm H} = 10^{24.5}$ cm^{-2}, with both cases $N_{\rm H} = 10^{23.5}$ and $10^{25.5}$ cm^{-2} producing a worse fit with $\Delta\chi^2 > 5.8$. According to Avni (1976), this implies that they can be rejected at the >98.5% confidence level. For the best-fitting case of $N_{\rm H} = 10^{24.5}$ cm^{-2}, the observed 2–8 keV band would be obscured by a factor of ~4, with respect to the intrinsic, unobscured emission.

Therefore, the X-ray spectrum of mid-IR excess sources is fully consistent with the presence of two major components: a star formation component (modeled here with a power-law emission of $\Gamma = 1.9$), plus a highly obscured AGN component with (average) $N_{\rm H} \sim 10^{24.5}$ cm^{-2}, i.e., mildly Compton-thick.

4.4. *Column Density and Mid-IR Luminosities*

The column density of obscuring gas can be independently estimated by exploiting the correlations between mid-IR and X-ray luminosities for AGNs, in the assumption that the mid-IR excess is entirely due to the AGN. The mid-IR excess sources to $K = 22$ in GOODS-S have average (median) 24 μm flux densities of 145 (131) μJy, while normal sources have average (median) 24 μm flux densities of 41 (27) μJy, consistent with the ongoing SFR on the basis of local correlations. We have computed for all galaxies the 24 μm flux densities expected for their $\rm SFR_{UV,corr}$ on the basis of Chary & Elbaz (2001) models and compared to the observed 24 μm flux densities. We find also in this way that for mid-IR excess galaxies the average (median) excess flux density is 100 (80) μJy. The ratio of 24 μm excess flux density to the total 24 μm flux density is found to be 69% (68%) on average (median). Therefore, we infer that the typical excess flux density is ≈80–100 μJy and that the AGN is contributing typically some $\frac{2}{3}$ of the observed 24 μm flux density in these mid-IR excess galaxies. These figures imply a ratio of 24 μm flux density to hard X-ray flux of $\sim 2 \times 10^{15}$ in the mJy (ergs s^{-1} cm^{-2})$^{-1}$ units used by Rigby et al. (2004). According to Rigby et al. (2004), based on the local AGN templates from Silva et al. (2004) with a range of obscuration, such large ratios at $z = 2$ would imply column densities $N_{\rm H} \gg 10^{24}$ cm^{-2}, or substantially Compton-thick sources. Using the observed correlations between the AGN mid-IR light and unobscured hard X-ray light from Lutz et al. (2004), which appear to hold independently of obscuration at least to $N_{\rm H} \sim 10^{25}$ cm^{-2}, we estimate that unobscured AGNs would contribute only ≈3–10 μJy at 24 μm for $z = 2$ given their 2–8 keV X-ray fluxes. In order to match the Lutz et al. (2004) correlation, the 2–8 keV observed flux requires a correction factor of ≈10–15, i.e., higher than the factor of ~4 derived in the previous section, and potentially implying Compton-thick AGNs with $N_{\rm H} > 10^{25}$ cm^{-2}.

It is instructive also to compare to the properties of NGC 1068, an extremely obscured local starburst harboring a heavily Compton-thick AGN with $N_{\rm H} > 10^{25}$ cm^{-2}. If placed at $z = 2$, the NGC 1068 nucleus would have a hard-band X-ray flux of 7×10^{-18} ergs s^{-1} cm^{-2} and a 24 μm flux density of 25 μJy. This would give a mid-IR–to–X-ray ratio of $\sim 3.5 \times 10^{15}$ [mJy (ergs s^{-1} cm^{-2})$^{-1}$] fully comparable with (slightly larger than) that of the mid-IR excess $z = 2$ galaxies. Therefore, these $z = 2$ sources are consistent with being the high-redshift analogs of NGC 1068, with overall luminosity scaled up by a factor of ~5. The AGN emission of NGC 1068 is thought to be obscured by over a factor of 10, even in the 6–24 keV band (rest frame).

We conclude from the mid-IR to X-ray comparisons that the majority of AGNs shrouded inside massive mid-IR excess $z = 2$ galaxies are likely Compton-thick, with average $N_{\rm H} > 10^{24}$ cm^{-2}, perhaps even in excess of the estimate of $N_{\rm H} \sim 10^{24.5}$ cm^{-2} derived solely from the X-ray stacking, and possibly in some cases they have extreme obscuration with $N_{\rm H} \gtrsim 10^{25}$ cm^{-2}.

4.5. *Intrinsic AGN Luminosities*

A determination of the intrinsic X-ray luminosity is critical to assess the general implications of our findings, but unfortunately it is made difficult because the obscuration appears to be very high. For the best-fitting Gilli et al. (2007) mildly Compton-thick model having $N_{\rm H} = 10^{24.5}$ cm^{-2}, the *observed* 2–8 keV band is obscured by a factor of of ~4. Consistently using this model to derive 2–8 keV flux from the observed counts yields a flux larger by a factor of 1.7 than that reported in Table 1, computed for $\Gamma = 0.8$. Correspondingly, we estimate that the average, isotropic, unobscured 2–8 keV *rest-frame* luminosity of mid-IR excess galaxies is $L_{2-8\,\rm keV} \sim 10^{43}$ ergs s^{-1}. To give an idea of the uncertainty in the correction for obscuration, we find that for the Gilli et al. (2007) templates the luminosities would decrease by a factor of 2.9 for $N_{\rm H} = 10^{23.5}$ cm^{-2} and would increase by a factor of 3.5 for $N_{\rm H} = 10^{25.5}$ cm^{-2} (although we emphasize that the absorption correction for the case of $N_{\rm H} = 10^{25.5}$ cm^{-2} is highly dependent on the assumed reflection efficiency).

As a comparison, we can use the Lutz et al. (2004) correlation between unobscured X-ray luminosities and 6 μm luminosities for AGNs, which is found to be independent of obscuration and has a scatter for individual sources of about a factor of 3. The relationship between the X-ray and mid-IR emission is strongly dependent on the dust-covering factor around the central source, and hence a source with a large dust covering factor will be more mid-IR luminous than one with a smaller dust covering factor (see Alexander et al. 2005a). The average 24 μm excess flux density attributed to the AGN is converted to an average 8 μm luminosity of order $4 \times 10^{10}\ L_\odot$ for the ensemble of mid-IR excess objects. We estimate ~70% of this value for the typical 6 μm luminosity of our sources (based on typical SEDs; see also Fig. 4). From Figure 7 in Lutz et al. (2004) we would then estimate $L_{2-8\,\rm keV} \sim 4 \times 10^{43}$ ergs s^{-1}, a factor of 4 larger than that obtained directly from X-ray. In summary, plausible values for the typical rest-frame 2–8 keV unabsorbed luminosities of mid-IR excess galaxies appear to be within $(1–4) \times 10^{43}$ ergs s^{-1}.

This result can be cross-checked by looking at the X-ray luminosities of *individually* hard X-ray–detected AGNs in our GOODS samples of *BzK*-selected sources with $1.4 < z < 2.5$. If we are finding the heavily obscured, Compton-thick counterparts of the already known population of $z \sim 2$ relatively unobscured sources, we might expect that the Compton-thick sources should have typical luminosities similar to the known AGNs, based on AGN unification models (Antonucci 1993; Urry & Padovani 1995). In fact, we find that the average 2–8 keV rest-frame luminosity of *individually* hard X-ray-detected AGNs in our *K*-selected sample is about $L_{2-8\,\mathrm{keV}} \sim 3 \times 10^{43}$ ergs s^{-1}, neglecting obscuration corrections that are likely negligible in most of these cases. The individually X-ray–detected $z = 2$ AGNs have a sky (and thus space) density that is a factor of ~3 smaller than that of our mid-IR excess galaxies in GOODS-S. Given the estimated X-ray luminosities, the mid-IR excess galaxies are also consistent with the correlation between optical/near-IR and 2–10 keV rest-frame luminosities found by Brusa et al. (2005) for distant AGNs.

One might also hope to constrain the bolometric luminosities of the AGNs in our sample, although uncertainties in the AGN bolometric correction factors are currently large (see, e.g., discussions in Pozzi et al. 2007; Hopkins et al. 2007). Assuming an AGN bolometric correction derived from the Elvis et al. (1994) SED, from the 2–8 keV X-ray luminosity we estimate $L_{\mathrm{bol}}^{\mathrm{AGN}} \sim (3\text{–}12) \times 10^{44}$ ergs s^{-1}, or about $(0.8\text{–}3) \times 10^{11}\ L_{\odot}$. The large range reflects only the uncertainty in the derived 2–8 keV rest-frame luminosity discussed above, as we are neglecting the unknown uncertainty in the bolometric correction for these galaxies. If instead we start from the mid-IR excess, with a typical luminosity of $10^{11}\ L_{\odot}$, the Elvis et al. (1994) SED would predict a bolometric correction of a factor of 10, or $L_{\mathrm{bol}}^{\mathrm{AGN}} \sim 10^{12}\ L_{\odot}$. Given that our galaxies are heavily obscured in X-rays to a similar degree, it may be more appropriate to use the mid-IR bolometric correction for the NGC 1068 nucleus, which is a factor of 3. This would lead us to estimate $L_{\mathrm{bol}}^{\mathrm{AGN}} \sim 3 \times 10^{11}\ L_{\odot}$. So, we are left with a plausible range spanning $(0.8\text{–}3) \times 10^{11}\ L_{\odot}$, although a value as high as $10^{12}\ L_{\odot}$ cannot be completely excluded at this stage. Admittedly, a very large uncertainty affects the estimated AGN bolometric luminosity.

From the ongoing star formation activity we estimate $L_{\mathrm{bol}}^{\mathrm{SF}} \sim 5 \times 10^{11}\ L_{\odot}$ for the typical mid-IR excess object, comparable to the bolometric luminosity of the AGN.

5. IMPLICATIONS

5.1. *The Sky and Space Density*

The main result of our study is the uncovering of a large population of Compton-thick AGNs at $z \sim 2$. We characterize here the abundance of this population. The sky density of the mid-IR excess AGNs in the GOODS-S field is ~0.7 arcmin^{-2} to $K < 22$ (59 sources in a 5.5′ radius region), after correcting for the 10% incompleteness in our sample due to the requirement of nonblended IRAC photometry (see Paper I). This estimate could increase by a factor of ~2, accounting for the sources that we excluded from the analysis not being able to properly measure for those either $\mathrm{SFR}_{\mathrm{mid\text{-}IR+UV}}$ or $\mathrm{SFR}_{\mathrm{UV,corr}}$ in equation (1) (which requires a well-measured UV slope and 24 μm detection, mainly; see § 2). As the excluded sources lacking 24 μm detections are less likely to be mid-IR excess galaxies, we conservatively correct the sky densities only by a factor of 1.3, to account for the overall fraction of red star-forming galaxies that were excluded from the analysis for not having a well-measured UV slope. This implies a sky density of 0.9 arcmin^{-2}, or some 3200 deg^{-2}. Using the volume within $1.4 < z < 2.5$ (see Fig. 2 in Paper I), we infer a space density of 2.6×10^{-4} Mpc^{-3} for the adopted ΛCDM cosmology.

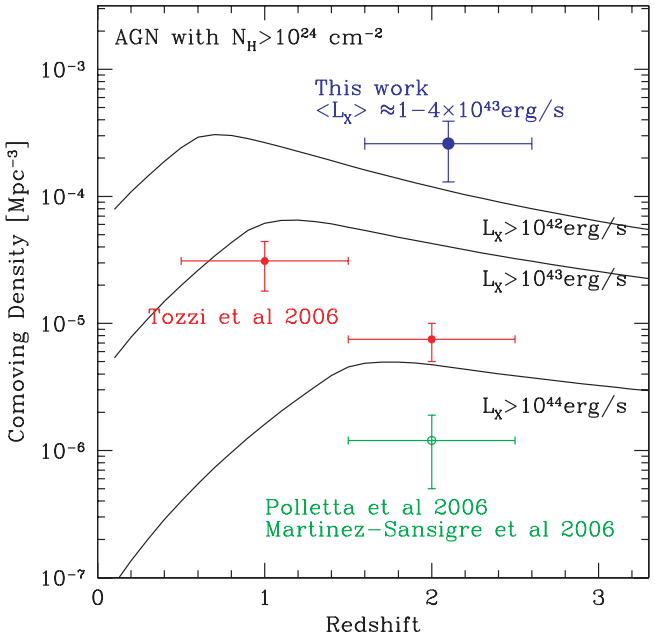

FIG. 10.—Space density of Compton-thick AGNs. The blue circle is our $z = 2.1$ estimate, where we allow for a factor of 2 uncertainty. The red circles are taken from Tozzi et al. (2006), based on direct *Chandra* detections in GOODS-S. The green circles show the density that we crudely estimate for the survey of Polletta et al. (2006) and Martínez-Sansigre et al. (2006), accounting in the latter case for completeness correction due to their radio preselection. The lines show the predictions of the background synthesis model of Gilli et al. (2007), as a function of the limiting X-ray luminosity.

We are dealing with detections of *average* properties only (X-ray stacking), and there is likely a spread in luminosities and N_{H} among the sample. In principle, only a fraction of the stacked mid-IR excess sources might be contributing the detected hard X-ray flux, e.g., in the case of a large contamination of the mid-IR excess galaxy sample from galaxies with peculiar mid-IR SEDs that are otherwise powered by star formation. In that case, the space density of this obscured AGN population would be lower by the same fraction, and its average X-ray flux and luminosity would be proportionally higher. The contributing fraction cannot be too small, i.e., at least ≈0.5; otherwise, we would have detected directly most of these sources in our *Chandra* data. Also, the similarity in inferred X-ray luminosities of these $z = 2$ Compton-thick AGNs to individually detected $z = 2$ sources (§ 4.5) argues against a lower fraction since this would boost their intrinsic luminosities. With this caveat, we have included all mid-IR sources in the computation of the space density of Compton-thick AGN candidates assuming that the mid-IR excess is due to the AGN as discussed above. Relaxing this hypothesis would not substantially affect any of the implications that we derive from this work.

5.2. *The Predominance of Compton-thick AGNs at High Redshift*

It is interesting to compare the properties of this previously undetected population of obscured, Compton-thick AGNs to AGN populations already known. Over the same redshift range $1.4 \lesssim z \lesssim 2.5$, the sky density of mid-IR excess, Compton-thick AGNs is a factor of ~2 higher than that of X-ray sources individually detected in X-rays in GOODS-S (Zheng et al. 2004), a factor of

≈10 higher than X-ray–detected submillimeter-emitting galaxies (Alexander et al. 2003a), and ≈20 times higher than X-ray–undetected power-law AGN candidates (Donley et al. 2007).

We can assess the obscured-to-unobscured AGN ratio by comparing to the space density of unobscured AGNs selected in the soft band by Hasinger et al. (2005). For $L_X > 10^{42}$ ergs s^{-1}, they find a space density of $\sim(3–4)\times10^{-5}$ at $z = 2$, a factor of $\gtrsim5$ smaller than what we find for obscured mid-IR excess AGNs at the same redshift. This implies that the ratio of obscured to unobscured AGNs is larger than at least 5, and is probably much larger yet, consistently with the model expectations (e.g., Gilli et al. 2007). Comparing to the luminosity function for hard X-ray–selected AGNs at $z = 2$ (Ueda et al. 2003; La Franca et al. 2005), the Compton-thick sources that we have found have a space density that is larger by a factor of 2–3 than that of the sources already known and overall with similar luminosities. The difference would decrease if it is only a fraction of mid-IR excess sources that are hosting an X-ray–luminous AGN. A more detailed comparison is hampered by the uncertainties inherent in the detailed properties of our samples, as discussed in the previous sections. Overall, these results suggest that a dominant fraction of X-ray–luminous AGNs are heavily obscured, in general agreement with expectations.

It is also interesting to compare to previously known populations of Compton-thick AGNs. Tozzi et al. (2006) identify six Compton-thick AGNs with $N_H > 10^{24}$ at $1.5 < z < 2.5$, detected by *Chandra* in the full GOODS-S, which translates into a space density at least an order of magnitude lower than that inferred here for our mid-IR excess objects. A larger density of Compton-thick AGNs is directly detected at $z \sim 1$ by Tozzi et al. (2006), but this is still a factor of at least 3 lower than our estimate at $z = 2$ (Fig. 10). Overall, the space density of Compton-thick AGNs that we infer at $z = 2$ is reasonably consistent, within a factor of 2, with the predictions of the background synthesis model of Gilli et al. (2007; Fig. 10), when counting all the Compton-thick sources in the models with 10^{42} ergs s^{-1} $< L_X < 10^{44}$ ergs s^{-1}, which are found to have an average X-ray luminosity of $L_X = 1.3\times10^{43}$ that is similar indeed to that of our sources.[21] This large population of Compton-thick $z \sim 2$ AGNs has probably similar intrinsic properties to that found by Martínez-Sansigre et al. (2006), who select $z \sim 2$ AGNs as mid-IR bright sources with a radio detection and a faint IRAC counterpart. They have uncovered a population of AGNs with a sky density of ≈10 deg^{-2}, turning out to be heavily obscured sources in nearly all cases. Their AGNs are likely the tip of the iceberg of the population found here, given their sky density some 2 orders of magnitude lower than that of our sources, but much higher bolometric luminosities. Similarly, Polletta et al. (2006) find a population of luminous Compton-thick AGNs at $z \sim 2$ using *Spitzer*, with a sky density of about 25 deg^{-2}.

In parallel to this work, Fiore et al. (2007) detected a similar population of $z \sim 2$ obscured AGNs from X-ray stacking of galaxies with large 24 μm–to–optical flux ratios. Given their selection criteria, we expect that many of the Fiore et al. (2007) objects would classify as mid-IR excess galaxies.

5.3. *Contribution to the X-Ray Background*

Given an observed average hard X-ray flux of $\sim10^{-16}$ ergs s^{-1} cm^{-2} (calculated directly from the model in Fig. 9, which gives ~1.7 times higher flux than given in Table 1; see § 4.5) and the sky density of 3200 deg^{-2}, the mid-IR excess sources produce a background of 0.7 keV s^{-1} cm^{-2} sr^{-1} in the 2–8 keV band. This is a quite small contribution to the total background in this band, which is not surprising given that this band is almost completely resolved by direct detections of individual AGNs (at least up to ≈6 keV; Worsley et al. 2005, 2006). The relative contribution of these mid-IR excess sources increases toward higher energies, as these sources are strongly obscured.

As an example, we have tried to extrapolate the background flux emitted in the 10–30 keV band. Using the best-fitting Gilli et al. (2007) model with $N_H = 10^{24.5}$ cm^{-2}, we estimate that these sources would produce a background flux of about 1.2 keV s^{-1} cm^{-2} sr^{-1} in the 10–30 keV band. For the physically motivated SEDs described in Gilli et al. (2007) this prediction turns out to be only weakly dependent on the assumed N_H, for AGNs around the Compton-thick regime. However, for the X-ray spectral shape at the highest energies of NGC 1068 and NGC 6240 (Vignati et al. 1999), we would derive a contribution a factor of 2 larger than above, being flatter at the highest energies than the Gilli et al. (2007) models (on the other hand, e.g., the Circinus galaxy has a spectral shape even softer than the Gilli et al. [2007] models; Matt et al. 1999). These calculations are insensitive to the particular fraction of mid-IR excess galaxies that are actually X-ray emitters, as the dependence is only on the stacked X-ray fluxes.

The total background in the 10–30 keV band is estimated to be about 44 keV s^{-1} cm^{-2} sr^{-1}. On the basis of the Gilli et al. (2007) model, ≈70%–80% of the 10–30 keV background can be ascribed to the sources detected in the deepest X-ray surveys in the ≈0.5–10 keV band. Therefore, we conclude that this population of $z = 2$ Compton-thick AGNs can account for ~10%–25% of the *missing* background in the 10–30 keV band, i.e., of the fraction due to Compton-thick AGNs that are not individually detected in X-rays. This is in reasonably good agreement with Gilli et al. (2007) model calculations for the background in this energy range emitted by Compton-thick AGNs at $1.4 < z < 2.5$. The same models predict that most of the rest of the X-ray background is produced by similar AGNs at $z < 1.4$ (although Steffen et al. [2007] find marginal background contributions from X-ray–undetected MIPS galaxies with 24 μm flux density >80 μJy at $z \sim 1$). Our results suggest that the AGNs in these $z < 1.4$ galaxies could be identified from the presence of excess mid-IR emission.

5.4. *On the Coeval Growth of Black Holes and Bulges*

About 20%–25% of the $z \sim 2$ star-forming galaxies in GOODS with $K < 22$ (i.e., with stellar masses $\gtrsim10^{10}\,M_\odot$) have 24 μm excesses by more than 0.5 dex, with the fraction rising to 50%–60% for the most massive star-forming galaxies with $M > 4\times10^{10}\,M_\odot$ (Fig. 5). We have shown that this appears to be due to the presence of heavily obscured AGNs in these objects, indicating that heavily obscured AGN activity was widespread among star-forming galaxies and massive galaxies in general at $z = 2$. This is different from the local universe, where the fraction of massive galaxies containing an AGN is only a few percent (Kauffmann et al. 2004), supporting the idea that the BH growth from the most massive BHs must have been higher in the past (see Fig. 2 in Heckman et al. 2004). The AGN activity is likely connected, in some physical way, to the intense star formation activity. In fact, locally a comparably large fraction of LIRGs and ULIRGs contain AGNs with detectable mid-IR excess (Genzel et al. 1998; Yun et al. 1999; Tran et al. 2001; Laurent et al. 2000). Therefore, the relative fraction of AGNs in LIRGs and ULIRGs might not

[21] We emphasize that the space density of Compton-thick AGNs at $z = 2$ in the Gilli et al. (2007) models is constrained by the shape of the missing X-ray background and is uncertain by a factor of a few. This is because $z = 2$ Compton-thick AGNs in the models produce only a small fraction of the missing background (see § 5.3).

be strongly evolving, while the fraction of AGNs in massive star-forming galaxies evolves by a substantial factor. Quite obviously, this suggests that the epoch of major buildup of stellar mass in galaxies at $z \sim 2$ (e.g., Daddi et al. 2005b; Papovich et al. 2006; Franceschini et al. 2006) coincided with a major buildup phase of the central supermassive BHs, as appears to be the case in the submillimeter-emitting galaxy population (e.g., Alexander et al. 2005b; Borys et al. 2005). This supports the idea that the local correlations between BH and galaxy mass were naturally put in place by a concomitant formation. Is there evidence of such a parallel growth of stellar and BH mass in our sample of $z \sim 2$ galaxies?

The rate of BH growth in these objects can be estimated from their bolometric luminosities, as $L_{\rm bol} = \eta \dot{M}_{\rm BH} c^2$, with a typical energy conversion efficiency $\eta \approx 0.1$ (e.g., Marconi et al. 2004). Given the large uncertainty in the bolometric luminosities of the AGNs in mid-IR excess galaxies ($10^{11}\ L_\odot \lesssim L_{\rm bol} \lesssim 10^{12}\ L_\odot$), we infer that the average BH accretion rate is in the range $\dot{M}_{\rm BH} \sim (0.05\text{–}0.5)\eta_{0.1}^{-1}\ M_\odot\ {\rm yr}^{-1}$ (here $\eta_{0.1} = \eta/0.1$). The mid-IR excess sources are only $\sim\frac{1}{4}$ of the sample of massive star-forming galaxies (i.e., the growth in stellar mass is happening in a $\sim$4 times larger sample of galaxies that remain undetected in hard X-rays). The average BH accretion per galaxy may thus be close to $\frac{1}{4}$ of the above estimate. We are neglecting here the possible additional BH growth inside galaxies classified in our simplification as mid-IR normal and BH growth occurring inside individually X-ray–detected $z = 2$ AGNs. The latter term, from individually hard X-ray–detected AGNs inside $z = 2$ massive star-forming galaxies, would increase the BH growth budget by *at most* a factor of 2, and likely much less (see § 4.5). The massive star-forming galaxies in our full GOODS-S sample have average SFR $\sim 70\ M_\odot\ {\rm yr}^{-1}$ (from the UV and soft X-ray). Assuming explicitly here the more physical IMF of Kroupa (2001) or Chabrier (2003), and considering (for comparison to the local universe) that only some 70% of these stars will survive at $z = 0$, we get a ratio of $\dot{M}_{\rm BH}/{\rm SFR} \sim (0.35\text{–}3.5) \times 10^{-3} \eta_{0.1}^{-1}$.

The local BH-to-galaxy mass correlation implies $M_{\rm BH}/M_{\rm bulge} \approx 1.5 \times 10^{-3}$ (McLure & Dunlop 2001; Marconi et al. 2004; Ferrarese et al. 2006), within about a factor of 2 uncertainty. Although uncertain, our estimate of the relative growth rates brackets the observed BH-to-stellar mass ratio, which tantalizingly suggests that this population of mid-IR excess galaxies may indeed represent the major building phase of BHs in massive galaxies. It is in fact largely expected that massive and star-forming $z = 2$ galaxies are the progenitors of local spheroids and bulges (e.g., Daddi et al. 2004a, 2004b; Shapley et al. 2005; Adelberger et al. 2005; Kong et al. 2006).

From the space density of these sources and their BH accretion rate, the cosmic BH accretion rate density turns out to be 10^{-5} to $10^{-4}\ M_\odot\ {\rm yr}^{-1}\ {\rm Mpc}^{-3}$. This is a factor of $\sim$2.5–25 larger than the contribution estimated for $z \approx 2$ bright SMGs (Alexander et al. 2005b), which appear to represent the most extreme star-forming galaxies at this epoch; clearly, fainter submillimeter observations may reveal significantly more AGNs and BH growth and eventually overlap with the K-selected population investigated here (which have $S_{850\ \mu{\rm m}} \sim 1\text{–}1.5$ mJy; see Daddi et al. 2005b; Paper I). However, this accretion rate density is comparable to the contribution of luminous quasars at these epochs (e.g., Yu & Tremaine 2002; Alexander et al. 2005b; Croton et al. 2006). Integrating over the 2 Gyr time span corresponding to the $1.4 < z < 2.5$ redshift range, this would produce a local BH mass density of $(0.2\text{–}2) \times 10^5\ M_\odot\ {\rm Mpc}^{-3}$. Comparing to the estimate of $4.6 \times 10^5\ M_\odot\ {\rm Mpc}^{-3}$ for the local integrated BH mass density (Marconi et al. 2004), our estimate is about 5%–50% of the total. This is similar to the estimate that today's massive galaxies are forming most of their stars in the $1.4 < z < 2.5$ redshift range, accounting for $\approx$20% of all the stars in the local universe (Daddi et al. 2005b).

5.5. *AGN Duty Cycle*

The high incidence of AGNs inside massive star-forming galaxies, 20%–30% for the overall samples, directly implies that the AGN activity at the luminosity levels at which we detect it has a relatively long duty cycle, at most only 3–4 times shorter than that of star formation. If only a fraction of mid-IR excess galaxies are actually X-ray luminous, these estimates would be reduced by the same fraction. Accounting for individual X-ray detections of massive star-forming galaxies would instead marginally increase these estimates (§ 4.5).

In Paper I we show that massive star-forming galaxies with $M > 10^{11}\ M_\odot$ are generally ULIRGs with a duty cycle of at least 40% and an estimated time duration of at least 400 Myr. At these high masses the fraction of mid-IR excess sources reaches $\sim$50%. Therefore, our results suggest that this obscured AGN activity in massive ($M > 10^{11}\ M_\odot$) galaxies has a duty cycle of at least $\sim$20% and typical durations of at least 200 Myr. We emphasize that these figures are likely to be lower limits because, given the downsizing trends, actively *star-forming* galaxies are likely to represent a higher fraction of all massive galaxies at masses lower than $10^{11}\ M_\odot$ at $z = 2$ (i.e., the fraction of quiescent/passive galaxies likely increases rapidly with stellar mass at $z = 2$). This is consistent with the timescales inferred by Marconi et al. (2004).

It is also worth noting that the strong increase of the fraction of mid-IR excess galaxies with stellar mass (see Fig. 5) might imply that the duty cycle of AGN activity inside star-forming galaxies depends on stellar mass. This could actually be the ultimate reason for downsizing, i.e., the fact that massive elliptical galaxies are the first to stop their star formation activity (e.g., Cimatti et al. 2006; Bundy et al. 2006; Scarlata et al. 2007). With more massive systems being more likely to host an AGN, they indeed would be the first ones to turn passive if AGN activity is the preferred feedback channel for the quenching star formation. Kriek et al. (2007) have proposed a similar argument.

5.6. *Submillimeter Galaxies, Merging, and BH Growth*

It is relevant at this point to summarize the comparison between *BzK* galaxies, particularly the mid-IR excess objects, and the coevally selected SMGs, as this has possibly interesting implications for the triggering of BH and galaxy growth. We have discussed in § 5.4 that the BH accretion rate density at $z = 2$ is higher by roughly an order of magnitude in the mid-IR excess galaxies, over that found in SMGs. Estimates of the $z = 2$ SFR density also show that SMGs account for a similar share of the overall stellar mass growth. Compared to the mid-IR excess galaxies selected to $K < 22$, SMGs are much rarer (at least at bright submillimeter flux densities of $f_{850\ \mu{\rm m}} > 5$ mJy; e.g., Coppin et al. 2006), have stellar masses larger by roughly a factor of 2–3 (e.g., Greve et al. 2005), have SFRs about 1 order of magnitude higher ($\approx$700 $M_\odot\ {\rm yr}^{-1}$ vs. $\approx$70 $M_\odot\ {\rm yr}^{-1}$; Chapman et al. 2005; this paper), but have AGN luminosities that are quite similar (a few times 10^{43} ergs s^{-1}; Alexander et al. 2005a, 2005b; this paper). This can explain why generally the SMGs do not display a mid-IR excess over their bolometric luminosity inferred from radio (Pope et al. 2006; see also Menéndez-Delmestre et al. 2007; Valiante et al. 2007), as the mid-IR emission from the AGN is likely overshadowed by that from star formation. This also implies that the ratio of BH growth to stellar mass growth is higher in mid-IR excess galaxies than in SMGs. For the former, the

concurrent BH and stellar mass growth can account for the buildup of galaxies lying on the locally defined BH-spheroid mass relation, while this is likely not the case for the activity of SMGs (Alexander et al. 2005a, 2005b).

Submillimeter-bright galaxies are likely a *special* phase during the buildup of massive galaxies corresponding to both the highest SFRs and specific SFRs. They lie outside the stellar mass versus SFR correlation, as described in Paper I, in the same way that ULIRGs are outliers of the local stellar mass–to–SFR correlation. This is consistent with the idea that SMGs like local ULIRGs are triggered by major mergers, as inferred also on the basis of their morphologies (Conselice et al. 2003; Chapman et al. 2003), and as suggested also by the compact sizes of the starbursts observed in CO lines and in the radio (Tacconi et al. 2006; Bouche et al. 2007). Instead, the fact that *BzK* galaxies in general define a tight stellar mass–to–SFR relation argues against an important role of major mergers in triggering their activity. The long duty cycle of their SFR activity (Daddi et al. 2005b; Paper I) also supports this idea, while SMGs are thought to be comparably much shorted lived (e.g., Greve et al. 2005; but see also Swinbank et al. 2006).

Therefore, an important conclusion that one might derive from our results is that BH growth in galaxies appears more directly connected with relatively stable and long-lived star formation, despite being still at considerably high rates, rather than being predominantly associated with rare and short-lived major merger events. We notice that most models of coeval BH and galaxy growth and of AGN feedback postulate instead that major mergers are the most relevant events for BH growth and for triggering feedback (e.g., Di Matteo et al. 2005; Schawinski et al. 2006; Croton et al. 2006). Our result is, in fact, somewhat surprising given that mergers are known to be very efficient in channeling the gas toward the center of the galaxies. Major mergers are likely still required to justify the rapid morphological transition between massive high-z star-forming galaxies with irregular/disk morphologies and bulge-dominated systems (although perhaps disk instabilities might also play this game; Genzel et al. 2006), but it appears that a substantial fraction of the BH masses inside local massive galaxies might have been put in place outside such events.

6. AGN FEEDBACK VIA COMPTON HEATING?

The widespread presence of obscured AGNs lurking inside massive star-forming galaxies naturally leads to the question of their possible feedback effect on their host galaxies. Feedback from AGNs is widely believed to be the key factor for solving a major problem of galaxy formation models based on ΛCDM cosmology. In short, these models require an ad hoc mechanism to quench star formation in massive galaxies, which is empirically required to reproduce the observed color bimodality of galaxies, as well as the old ages of stars in early-type galaxies. Passively evolving elliptical galaxies are now known to be present in significant numbers at least up to $z \sim 2.5$ (Cimatti et al. 2004; McCarthy et al. 2004; Daddi et al. 2005a). As first shown by Granato et al. (2001, 2004), physically motivated semiempirical models of galaxy evolution implementing AGN feedback can successfully account for the existence of massive and passive galaxies already at early epochs (see also De Lucia et al. 2006; Springel et al. 2006; Croton et al. 2006; Bower et al. 2006; Kitzbichler & White 2006), as shown also in Paper I. Our results are consistent with the idea that potentially *all* $z = 2$ massive star-forming galaxies contain AGNs, and therefore the ad hoc mechanism advocated by the models appears at least to be plausible because the AGNs are indeed there. Therefore, it would be of great interest to find a direct observational connection between AGN activity and star formation quenching in massive galaxies.

We can imagine two ways that energy can be transferred from the AGN to the host interstellar medium (ISM), heating it up until it escapes from the galaxy in a wind. One is via (sub)relativistic jets, and their possible role in a similar context (suppression of galaxy *cooling flows*) has been invoked by, e.g., Binney & Tabor (1995). Alternatively (or in addition), the hard X-rays emitted by the AGN may produce Compton heating as they are absorbed by the ISM, again powering galactic winds (Ciotti & Ostriker 1997, 2007). AGN jets and accretion-related outflows are likely a major channel for mechanical feedback in distant galaxies. However, we cannot state anything new on the issue based on our sample of $z \sim 2$ galaxies and our results. We focus instead here on the latter option, as the likely Compton-thick nature of these AGNs indicates that Compton heating could indeed be taking place.

The large obscuration of the central BH implies that very high energy photons are heavily absorbed by the material surrounding the AGN, which can thus be efficiently heated. The typical star-forming galaxy in our GOODS-S sample has a stellar mass of $M \sim 3 \times 10^{10}\ M_{\odot}$, and the binding energy of the gas can be estimated to be of the order of $M_{\rm gas}\sigma_v^2 \approx 3 \times 10^{58} f_{\rm gas}$, where $f_{\rm gas}$ is the gas fraction of the galaxy's baryonic mass and σ_v is the velocity dispersion. The X-ray luminosity absorbed at high energies, e.g., >2 keV in the rest frame, is $\gtrsim 10^{43}$ ergs s^{-1}. These very high energy photons can efficiently heat the gas, through Compton scattering. Assuming, as a limiting case, that all the absorbed energy at >2 keV goes into extracting gas from the galactic potential well, and using $f_{\rm gas} = 0.1$, it would take only $\sim 3 \times 10^6$ yr to blow off the gas completely. Clearly, the efficiency is likely to be much lower, chiefly because the material in the BH surroundings can absorb and reradiate to lower energies most of the energy of the absorbed hard X-ray photons. The mid-IR excess itself testifies for (part of) the AGN energy output being indeed degraded. The energy available for feedback is the difference between the total hard X-ray energetic output of the AGN and the fraction of it that is reradiated at lower energies. Since both terms are affected by large uncertainties, estimating their difference would be affected by even larger uncertainties. Notwithstanding this limitation, the large unobscured luminosity in hard X-rays that we derive for these objects argues for the plausibility of a scenario in which Compton heating plays an important role in quenching star formation.

7. FUTURE PROSPECTS

We have discovered a substantial population of heavily obscured, Compton-thick AGNs, residing in a large fraction of massive star-forming galaxies at $z \sim 2$. We have shown that this result has important implications for BH galaxy evolution, but our analysis still leaves open many questions. There are two crucial points that will need to be addressed by future studies: a cleaner selection of mid-IR excess objects and an improved estimate of the obscuring column densities, hence of $L_{\rm X}^{\rm AGN}$ and $L_{\rm bol}^{\rm AGN}$.

For the selection, the main current limitation is that the fiducial SFR activity of the host galaxy, used to diagnose the presence of an excess at mid-IR bands, is derived from the UV. Due to the necessity of large (hence uncertain) reddening corrections, and in some cases of UV obscuration exceeding what can be inferred from the UV slope, this procedure is far from being ideal. A better procedure would be to derive a reliable measurement of the bolometric IR luminosity of the galaxy from long-wavelength observations and compare this to the mid-IR rest-frame luminosity. The availability of ALMA, SCUBA2, and especially *Herschel*

observations in the near future should all substantially help with this task, providing much better multiwavelength SEDs for the dust emission, from mid-IR wavelengths through the far-IR peak and beyond. With such a detailed SED, one could try to disentangle the cold dust and the warm dust emission, due to, respectively, star formation and AGN heating.

Measuring reliable values for $N_{\rm H}$, determining accurately what fraction of mid-IR excess sources are Compton-thick, and perhaps also detecting individually these sources would require extremely sensitive observations. With *Chandra* this could require an ultradeep integration, of the order of 5–10 Ms, to allow one to detect some of the brightest objects. Perspectives also look promising for the next generation of X-ray satellites currently under discussion, such as *XEUS* (Bavdaz et al. 2006); if realized with a fairly high angular resolution ($\sim 2''$–$3''$), *XEUS* would be ideally suited to X-ray spectroscopy of these X-ray–faint AGNs. Rest-frame optical spectroscopy can also provide insights by looking for luminous high-excitation emission lines such as [O III] λ5007.

Mid-IR spectroscopy will also be crucial to improve our understanding of these sources. We have not as yet explicitly demonstrated that AGN emission does account for the entirety of the mid-IR excess flux density. Our analysis cannot exclude the possibility that intrinsically different mid-IR SED properties, e.g., anomalously strong polycyclic aromatic hydrocarbons (PAHs), exist in a fraction of $z = 2$ galaxies, with the mid-IR still powered by SFR. This might be related to the presence of different SFR modes, rare or nonexistent by $z < 1$, a result that would be quite interesting on its own. Clearly, the ideal means to obtain a direct diagnostic of the cause of the 24 μm excess would be to perform spectroscopy at these wavelengths with *Spitzer* and *AKARI*. Given that the typical mid-IR excess galaxy is highly star forming, we do expect to see PAH features in a large majority of the mid-IR excess galaxies. However, if the mid-IR excess is directly produced by the AGN, we should detect also an important contribution from AGN continuum in most of the mid-IR spectra, lowering the equivalent width of the PAH emission features. As mid-IR excess objects even at $z \sim 2$ are relatively bright at 24 μm, with flux densities often in excess of 100–200 μJy, the observations are feasible and useful spectra are already available in the *Spitzer* archive, although their analysis exceeds the scope of the present paper.

8. SUMMARY AND CONCLUSIONS

We have studied the nature of a population of $z \sim 2$ galaxies that displays a marked excess flux density at mid-IR wavelengths, over that expected to arise from just normal star formation activity as estimated from their rest-frame UV. The examined sample includes over 600 *K*-selected $z \sim 2$ galaxies in the two GOODS fields (with 25% of them having spectroscopic redshifts), with multiwavelength information including data in UV, optical, near-IR, *Spitzer* IRAC (3.6–8.0 μm bands), *Spitzer* MIPS (24 and 70 μm bands), SCUBA, VLA 1.4 GHz, and X-ray from *Chandra*. This sample has been cleaned by all known AGNs, identified via their *Chandra* 2–8 keV X-ray emission and/or by the presence of a power-law SED over the IRAC bands. The major results of this work can be summarized as follows:

1. Roughly 20%–30% of the massive star-forming galaxies at $z \sim 2$, selected down to $K < 22$, display a mid-IR excess larger than about a factor of 3, which we classify as "mid-IR excess galaxies." This fraction increases rapidly with the stellar mass of the galaxies, reaching $\sim$50%–60% for $M > 4 \times 10^{10}\ M_{\odot}$. We have shown that our results do not strongly depend on the exact threshold used for defining these mid-IR excess galaxies.

2. This population of mid-IR excess galaxies is at slightly higher average redshift than normal galaxies ($\langle z \rangle = 2.1$ vs. 1.9), but overall the two redshift distributions are similar. This population becomes dominant at the highest 8 μm (rest frame) luminosities [for $L(8\ \mu{\rm m}) > 10^{11}\ L_{\odot}$] that we accurately derive at $z \sim 2$ from *Spitzer* MIPS 24 μm flux densities. Relatively shallow surveys with *Spitzer* MIPS of the $z \sim 2$ universe are thus the ones that are proportionally most affected by the presence of mid-IR excess galaxies.

3. Mid-IR excess sources have redder $K - 5.8$ μm colors than normal galaxies, reflecting different intrinsic SEDs in the optical to near-IR rest frame, that cannot be attributed to mere redshift effects. For these mid-IR excess sources, the peak of the stellar-dominated part of the SED is longward of the canonical 1.6 μm rest frame. We interpret this as evidence for the presence of a warm dust AGN contribution to the continuum in these sources, consistent also with the finding that the excess flux density seems to become weaker beyond 20 μm rest frame, based on *Spitzer* 70 μm observations.

4. This excess AGN component over the near-IR rest frame will likely bias the estimates of stellar masses and photometric redshifts for some of the $z \sim 2$ galaxies, when including IRAC photometry in the SEDs. However, we quantify the effect on the derived photometric redshifts to be only at the level of 2%–3% in $(1 + z)$, for the mid-IR excess sources.

5. Stacking of *Chandra* X-ray data reveals a strong dichotomy in the two populations: the normal sources have a soft spectrum, consistent with star formation in both 0.5–2 and 2–8 keV bands. Contrary to them, mid-IR excess objects exhibit a much harder spectrum, unambiguously showing the presence of highly obscured AGNs inside these sources.

6. We use a variety of methods to infer $N_{\rm H}$, the column density of the absorbing material along the line of sight. Our best estimate suggests typical obscuration of $N_{\rm H} = 10^{24.5}$ cm^{-2}, derived from the X-ray spectrum after accounting for the X-ray emission due to star formation. As a result, we infer that the majority of the mid-IR excess galaxies are likely to host a Compton-thick AGN.

7. This previously unknown population of AGNs has typical X-ray luminosity of $(1$–$4) \times 10^{43}$ ergs s^{-1} in the 2–8 keV rest-frame band. We infer a range for the bolometric luminosity of 10^{11}–$10^{12}\ L_{\odot}$. This is comparable to the bolometric luminosities of their host galaxies, as due to star formation, for which we estimate a typical value of $\sim 5 \times 10^{11}\ L_{\odot}$.

8. The sky density of Compton-thick AGNs inside massive star-forming galaxies to $K < 22$ is $\sim$3200 deg^{-2}, and their space density is $\sim 2.6 \times 10^{-4}$ Mpc^{-3}. Their space density is higher than that of all AGNs already known at $z = 2$, and much higher than that of previously known Compton-thick populations at high redshifts. The space density of Compton-thick AGNs that we derive agrees reasonably well with that predicted by the background synthesis models of Gilli et al. (2007).

9. Despite their large space density, we extrapolate that this population can account for only about 10%–25% of the *missing* X-ray background in the observed 10–30 keV band, in agreement again with the prediction of Gilli et al. (2007). Most of the high-energy background still to be resolved is likely inside similar sources but residing at $z \lesssim 1.4$ rather than at $z \sim 2$.

10. The widespread presence of obscured AGNs inside massive star-forming galaxies at $z \sim 2$ seems to quite naturally account for the concurrent growth of the BH together with the stellar

mass of the hosting galaxies. Within quite large quantitative uncertainties, this picture is consistent with these objects approaching the local values for the ratios between the mass of central BHs and that of their hosting bulges.

11. A relatively long duty cycle for the AGN activity at $z = 2$, only a factor of 3–4 lower than that of star formation activity, is suggested by the widespread presence of AGNs that appear to be present among massive star-forming galaxies.

12. Comparing to submillimeter-selected galaxies (SMGs), we find that BHs are growing faster in mid-IR excess galaxies, relatively to the ongoing SFR, and their integrated contribution to the BH accretion rate density is also larger. This suggests that BH growth in massive galaxies is taking place outside major merger events.

13. The large, increasing incidence of Compton-thick AGNs with stellar mass, along with the energy deposition provided by the absorption of the hard X-ray photons, suggests that these objects may be responsible for the AGN feedback eventually leading to the termination of the star formation activity, and doing so beginning with the most massive galaxies as in the *downsizing* scenario. Although existing data do not allow one to firmly prove this tantalizing possibility, we show that the involved energetics is consistent with this picture.

14. We finally discuss future prospects for improving our still limited understanding of the properties of mid-IR excess galaxies and Compton-thick AGNs at high redshift. The crucial and obvious required next step is the full construction of their SED, including ALMA, SCUBA2, and *Herschel* facilities as they become available, as well as of their *spectral* mid-IR properties, via *Spitzer* IRS and *AKARI* spectroscopy. Extremely deep *Chandra* (5–10 Ms) exposures would be required to directly detect some of these Compton-thick AGNs.

In summary, we have uncovered a major population of luminous and obscured $z = 2$ AGNs, previously largely unknown. With AGN and star formation activity in massive galaxies peaking at $z \sim 2$, this newly detected population of Compton-thick AGNs appears to be an excellent candidate for playing a major role both for establishing the BH-bulge mass relation and for providing the feedback necessary to discontinue further star formation in massive galaxies.

We thank the rest of the GMASS team for allowing us to use the still unpublished spectroscopic redshifts, as well as the many other members of the GOODS team, who have helped to make these observations possible. We are grateful to Emily MacDonald, Daniel Stern, and Hy Spinrad for collecting some of the redshifts used in this work. We thank Gianni Zamorani and Susanne Madden for useful comments and discussions. E. D. gratefully acknowledges NASA support (at the beginning of this work) through the *Spitzer* Fellowship Program, award 1268429. D. M. A. thanks the Royal Society for funding. R. G. acknowledges financial support from the Italian Space Agency (ASI) under the contract ASI-INAF I/023/05/0. W. N. B. acknowledges *Spitzer Space Telescope* grant 1278940. J. K. acknowledges financial support from the German Science Foundation (DFG) under contract SFB-439. Support for this work, part of the *Spitzer Space Telescope* Legacy Science Program, was provided by NASA, contract 1224666 issued by the JPL, Caltech, under NASA contract 1407.

REFERENCES

Adelberger, K. L., Erb, D. K., Steidel, C. C., Reddy, N. A., Pettini, M., & Shapley, A. E. 2005, ApJ, 620, L75
Alexander, D. M., Bauer, F. E., Chapman, S. C., Smail, I., Blain, A. W., Brandt, W. N., & Ivison, R. J. 2005a, ApJ, 632, 736
Alexander, D. M., Smail, I., Bauer, F. E., Chapman, S. C., Blain, A. W., Brandt, W. N., & Ivison, R. J. 2005b, Nature, 434, 738
Alexander, D. M., et al. 2003a, AJ, 125, 383
———. 2003b, AJ, 126, 539
Alonso-Herrero, A., et al. 2006, ApJ, 640, 167
Antonucci, R. 1993, ARA&A, 31, 473
Armus, L., et al. 2007, ApJ, 656, 148
Avni, Y. 1976, ApJ, 210, 642
Barger, A. J., Cowie, L. L., & Wang, W.-H. 2007, ApJ, 654, 764
Bavdaz, M., et al. 2006, Proc. SPIE, 6266, 51
Binney, J., & Tabor, G. 1995, MNRAS, 276, 663
Borys, C., Smail, I., Chapman, S. C., Blain, A. W., Alexander, D. M., & Ivison, R. J. 2005, ApJ, 635, 853
Bouche, N., et al. 2007, ApJ, in press (arXiv: 0706.2656)
Bower, R. G., et al. 2006, MNRAS, 370, 645
Brandt, W. N., & Hasinger, G. 2005, ARA&A, 43, 827
Brandt, W. N., Hornschemeier, A. E., Schneider, D. P., Alexander, D. M., Bauer, F. E., Garmire, G. P., & Vignali, C. 2001, ApJ, 558, L5
Brusa, M., et al. 2005, A&A, 432, 69
Bundy, K, et al. 2006, ApJ, 651, 120
Calzetti, D., et al. 2000, ApJ, 533, 682
Chabrier, G. 2003, ApJ, 586, L133
Chapman, S. C., Blain, A. W., Smail, I., & Ivison, R. J. 2005, ApJ, 622, 772
Chapman, S. C., Windhorst, R., Odewahn, S., Yan, H., & Conselice, C. 2003, ApJ, 599, 92
Chartas, G., Brandt, W. N., Gallagher, S. C., & Proga, D. 2007, AJ, 133, 1849
Chary, R., & Elbaz, D. 2001, ApJ, 556, 562
Chary, R.-R., Teplitz, H. I., Dickinson, M. E., Koo, D. C., Le Floc'h, E., Marcillac, D., Papovich, C., & Stern, D. 2007, ApJ, 665, 257
Cimatti, A., Daddi, E., & Renzini, A. 2006, A&A, 453, L29
Cimatti, A., et al. 2004, Nature, 430, 184
Ciotti, L., & Ostriker, J. P. 1997, ApJ, 487, L105
———. 2007, ApJ, 665, 1038
Comastri, A., Setti, G., Zamorani, G., & Hasinger, G. 1995, A&A, 296, 1
Conselice, C. J., Chapman, S. C., & Windhorst, R. A. 2003, ApJ, 596, L5
Coppin, K., et al. 2006, MNRAS, 372, 1621
Croom, S. M., Smith, R. J., Boyle, B. J., Shanks, T., Miller, L., Outram, P. J., & Loaring, N. S. 2004, MNRAS, 349, 1397
Croton, D. J., et al. 2006, MNRAS, 365, 11
Daddi, E., Cimatti, A., Renzini, A., Fontana, A., Mignoli, M., Pozzetti, L., Tozzi, P., & Zamorani, G. 2004a, ApJ, 617, 746
Daddi, E., et al. 2004b, ApJ, 600, L127
———. 2005a, ApJ, 626, 680
———. 2005b, ApJ, 631, L13
———. 2007, ApJ, 669, 156 (Paper I)
Dale, D. A., et al. 2006, ApJ, 646, 161
De Lucia, G., Springel, V., White, S. D. M., Croton, D., & Kauffmann, G. 2006, MNRAS, 366, 499
Di Matteo, T., Springel, V., & Hernquist, L. 2005, Nature, 433, 604
Donley, J. L., Rieke, G. H., Pérez-González, P. G., Rigby, J. R., & Alonso-Herrero, A. 2007, ApJ, 660, 167
Elbaz, D., et al. 2007, A&A, 468, 33
Elvis, M., et al. 1994, ApJS, 95, 1
Fabian, A. C., & Iwasawa, K. 1999, MNRAS, 303, L34
Ferrarese, L., & Merritt, D. 2000, ApJ, 539, L9
Ferrarese, L., et al. 2006, ApJ, 644, L21
Fiore, F., et al. 2007, ApJ, in press (arXiv: 0705.2864)
Franceschini, A., et al. 2006, A&A, 453, 397
Frayer, D. T., et al. 2006, ApJ, 647, L9
Gebhardt, K., et al. 2000, ApJ, 539, L13
Genzel, R., et al. 1998, ApJ, 498, 579
———. 2006, Nature, 442, 786
Giacconi, R., et al. 2002, ApJS, 139, 369
Giavalisco, M., et al. 2004, ApJ, 600, L93
Gilli, R., Comastri, A., & Hasinger, G. 2007, A&A, 463, 79
Gilli, R., Salvati, M., & Hasinger, G. 2001, A&A, 366, 407
Granato, G. L., De Zotti, G., Silva, L., Bressan, A., & Danese, L. 2004, ApJ, 600, 580
Granato, G. L., Silva, L., Monaco, P., Panuzzo, P., Salucci, P., De Zotti, G., & Danese, L. 2001, MNRAS, 324, 757
Greve, T. R., et al. 2005, MNRAS, 359, 1165
Hasinger, G. 2004, Nucl. Phys. B, 132, 86

Hasinger, G., Miyaji, T., & Schmidt, M. 2005, A&A, 441, 417
Heckman, T. M., Kauffmann, G., Brinchmann, J., Charlot, S., Tremonti, C., & White, S. D. M. 2004, ApJ, 613, 109
Hickox, R. C., & Markevitch, M. 2007, ApJ, 661, L117
Hopkins, P. F., Richards, G. T., & Hernquist, L. 2007, ApJ, 654, 731
Hornschemeier, A. E., Heckman, T. M., Ptak, A. F., Tremonti, C. A., & Colbert, E. J. M. 2005, AJ, 129, 86
Kauffmann, G., White, S. D. M., Heckman, T. M., Ménard, B., Brinchmann, J., Charlot, S., Tremonti, C., & Brinkmann, J. 2004, MNRAS, 353, 713
Kitzbichler, M. G., & White, S. D. M. 2006, MNRAS, 366, 858
Kong, X., et al. 2006, ApJ, 638, 72
Kormendy, J., & Richstone, D. 1995, ARA&A, 33, 581
Kriek, M., et al. 2007, ApJ, 669, 776
Krivonos, R., Vikhlinin, A., Churazov, E., Lutovinov, A., Molkov, S., & Sunyaev, R. 2005, ApJ, 625, 89
Kroupa, P. 2001, MNRAS, 322, 231
Lacy, M., et al. 2004, ApJS, 154, 166
La Franca, F., et al. 2005, ApJ, 635, 864
Laurent, O., Mirabel, I. F., Charmandaris, V., Gallais, P., Madden, S. C., Sauvage, M., Vigroux, L., & Cesarsky, C. 2000, A&A, 359, 887
Lutz, D., Maiolino, R., Spoon, H. W. W., & Moorwood, A. F. M. 2004, A&A, 418, 465
Magorrian, J., et al. 1998, AJ, 115, 2285
Marconi, A., Risaliti, G., Gilli, R., Hunt, L. K., Maiolino, R., & Salvati, M. 2004, MNRAS, 351, 169
Marshall, F. E., Boldt, E. A., Holt, S. S., Miller, R. B., Mushotzky, R. F., Rose, L. A., Rothschild, R. E., & Serlemitsos, P. J. 1980, ApJ, 235, 4
Martínez-Sansigre, A., Rawlings, S., Lacy, M., Fadda, D., Jarvis, M. J., Marleau, F. R., Simpson, C., & Willott, C. J. 2006, MNRAS, 370, 1479
Matt, G., et al. 1999, A&A, 341, L39
McCarthy, P. J., et al. 2004, ApJ, 614, L9
McLure, R. J., & Dunlop, J. S. 2001, MNRAS, 327, 199
Menéndez-Delmestre, K., et al. 2007, ApJ, 655, L65
Noeske, K. G., et al. 2007, ApJ, 660, L43
Papovich, C., et al. 2006, ApJ, 640, 92
———. 2007, ApJ, 668, 45
Peng, C. Y., Ho L. C., Impey, C. D., & Rix, H.-W. 2002, AJ, 124, 266
Persic, M., & Rephaeli, Y. 2002, A&A, 382, 843
Persic, M., Rephaeli, Y., Braito, V., Cappi, M., Della Ceca, R., Franceschini, A., & Gruber, D. E. 2004, A&A, 419, 849
Polletta, M. d. C., et al. 2006, ApJ, 642, 673
Pope, A., Borys, C., Scott, D., Conselice, C., Dickinson, M., & Mobasher, B. 2005, MNRAS, 358, 149
Pope, A., et al. 2006, MNRAS, 370, 1185
Pozzi, F., et al. 2007, A&A, 468, 603
Ranalli, P., Comastri, A., & Setti, G. 2003, A&A, 399, 39
Rigby, J. R., et al. 2004, ApJS, 154, 160
Sawicki, M. 2002, AJ, 124, 3050
Scarlata, C., et al. 2007, ApJS, 172, 494
Schawinski, K., et al. 2006, Nature, 442, 888
Schmidt, M. 1968, ApJ, 151, 393
Shapley, A., et al. 2005, ApJ, 626, 698
Silk, J., & Rees, M. J. 1998, A&A, 331, L1
Silva, L., Maiolino, R., & Granato, G. L. 2004, MNRAS, 355, 973
Spergel, D. N., et al. 2007, ApJS, 170, 377
Springel, V., Di Matteo, T., & Hernquist, L. 2005, ApJ, 620, L79
Springel, V., Frenk, C. S., & White, S. D. M. 2006, Nature, 440, 1137
Steffen, A. T., Brandt, W. N., Alexander, D. M., Gallagher, S. C., & Lehmer, B. D. 2007, ApJ, 667, L25
Stern, D., et al. 2005, ApJ, 631, 163
Swinbank, A. M., Chapman, S. C., Smail, I., Lindner, C., Borys, C., Blain, A. W., Ivison, R. J., & Lewis, G. F. 2006, MNRAS, 371, 465
Tacconi, L. J., et al. 2006, ApJ, 640, 228
Tozzi, P., et al. 2006, A&A, 451, 457
Tran, Q. D., et al. 2001, ApJ, 552, 527
Treister, E., et al. 2004, ApJ, 616, 123
Ueda, Y., Akiyama, M., Ohta, K., & Miyaji, T. 2003, ApJ, 598, 886
Urry, C. M., & Padovani, P. 1995, PASP, 107, 803
Valiante, E., Lutz, D., Sturm, E., Genzel, R., Tacconi, L. J., Lehnert, M. D., & Baker, A. J. 2007, ApJ, 660, 1060
Vignati, P., et al. 1999, A&A, 349, L57
Worsley, M. A., Fabian, A. C., Bauer, F. E., Alexander, D. M., Brandt, W. N., & Lehmer, B. D. 2006, MNRAS, 368, 1735
Worsley, M. A., et al. 2005, MNRAS, 357, 1281
Yun, M. S., Hibbard, J. E., Condon, J. J., & Reddy, N. 1999, Ap&SS, 266, 29
Yu, Q., & Tremaine, S. 2002, MNRAS, 335, 965
Zheng, W., et al. 2004, ApJS, 155, 73